Analysis of Switching Schemes for 3-Phase Static AC-DC Converter

Md. Nurul Amin Chowdhury

A Thesis

in

The Department

of

Electrical Engineering

Presented in Partial Fulfilment of the Requirements
for the degree of Master of Engineering at
Concordia University
Montréal, Québec, Canada

May 1984

ABSTRACT

Analysis of Switching Schemes for 3-Phase Static AC-DC Converter

Md. Nurul Amin Chowdhury

The performances of 3-phase AC-DC converters with different switching schemes are compared. Emphasis is given on the utilisation of the converter in selecting the switching functions. A conventional six-switch converter structure is used throughout the study. The input and output current and output voltage are determined by frequency domain analysis. An unbalance in a 3-phase AC supply voltage produces non-characteristic harmonic components in the input current of converter. The performance of 3-phase AC-DC converters are compared for both balanced and unbalanced supply voltage conditions. A detailed harmonic analysis is done to determine the order and magnitude of harmonic components present in the input and output of converters with different switching schemes. The suitability of different switching schemes are determined depending on operating criteria. The study will be useful in determining the effects of different switching schemes and supply unbalances on the distortion factor, total harmonic distortion, input power factor and lower order harmonics of the converter. It also gives comprehensive idea about minimizing and/or maximizing certain criterion for the converters and also about filtering requirements with different switching schemes.

ACKNOWLEDGEMENTS

The author wishes to express his heartfelt gratitude to Professor M.H. Rashid for suggesting the problem and for his guidance and assistance during the entire preparation of this thesis. The author is gratefull to Dr. A. Antoniou, former Chairman and Dr. J.G. Giguere, acting Chairman of Electrical Engineering Department for providing excellent research facilities in the department.

Thanks are due to Marie Berryman for typing the thesis.

This work was supported by the National Science and Engineering Research Council of Canada under a grant (A 1744), awarded to Professor M.H. Rashid.

TABLE OF CONTENTS

PAGE

NOTE: All computer programs related to this thesis are available with Dr. M.H. Rashid, Department of Electrical Engineering, Concordia University.

LIST OF SYMBOLS

A_c	Amplitude of carrier waveform
A_r	Amplitude of reference waveform
E_1, E_2, E_3	Peak value of the phase voltage, V
E_c	Counter emf of the load circuit, V
f	Supply frequency, Hz
f_N	Normalised frequency
H_n	nth harmonic component of switching function
i_i	Instantaneous input current, A
i_o	Instantaneous output current, A
I_i	RMS value of input current, A
$I_{i,1}$	RMS value of fundamental input current, A
I_{dc}	Average output current, A
I_n	Peak value of the nth harmonic component of output current, A
I_{G_n}	Gating signal of nth semiconductor switch
L	Load inductance, H
M	Modulation index
N_p	Number of pulses per half cycle
R	Load resistance, Ω
$S(\theta)$	Switching function

T_n	nth switching angle
V_{dc}	Average output voltage, V
V_{an}, V_{bn}, V_{cn}	RMS value of input phase voltage
V_{ab}, V_{bc}, V_{ca}	RMS value of input line voltage
v_{om}	Instantaneous mth harmonic component of output voltage, V
V_N	Normalised average output voltage
X_n	RMS value of the nth harmonic component
α	Delay angle, rad
β_n	Phase of the nth harmonic component of output current, rad
ψ_n	Phase of the nth harmonic component of switching function, rad
ϕ_1, ϕ_2, ϕ_3	Phase angle of the phase voltages, rad

LIST OF FIGURES

CHAPTER 1

INTRODUCTION

1.1 Review

Three phase AC-DC Static power converters are extensively used for power conversion. These static power converters are nonlinear. They produce nonsinusoidal current on the power system. Initially there were a very few AC-DC converter loads on a given bus. The distortions were not so severe and no serious problems were reported other than computer malfunction [1]. Today the converter load is a substantial portion of the total system power requirements [1]. They generate significant amount of harmonic current into the system thereby introducing a) increased losses and b) interference with communication lines.

The resulting power factor of an AC-DC converter is usually poor. From economic and line voltage regulation point of view it is required to improve the overall system power factor. This power factor improvement was achieved by using shunt capacitor. When these capacitor banks were used, problems of voltage and current harmonics due to these capacitor and other system equipment became dominant [2,3]. For normal static power converter operation the circuit parameters of converter do not combine with system parameters to be resonant at any characteristic harmonic [2]. The natural frequencies of power circuits are in the kilohertz range. But when the capacitors are added to the system the resonance frequencies may fall within the range of harmonic frequencies encountered with static power converters. In actual power systems which uses power factor correction capacitors, series or parallel resonance

or a combination of both may occur if the resonant point becomes close to one of the frequencies generated by static power converter [2-5]. The result is excessive harmonic current flow or excessive harmonic overvoltages.

The recent problems involve the use of sophisticated electrical and electronic equipment which are very sensitive to harmonics in power lines [2,3,5]. Metering and instrumentation are also affected by these harmonic currents. Carrier system that control remote devices can produce erroneous operation if the generated harmonics are close to the carrier signal [7]. In future the static power converter will make harmonic distortion the only important problem in static power conversion [6].

The harmonic currents generated by static power converter can be suppressed by using a) proper input/output filters and b) proper switching function for the switches of the converter. The filter adds extra cost and weight to the converter. It is preferable to use a proper switching function so that the harmonics generated by power conversion device alone is reduced [9-11] and then to use a comparatively smaller size filter.

Besides the characteristic harmonics of AC-DC converters other non-characteristic harmonics are produced due to imperfections such as:

a. unbalanced transformer impedances,
b. unbalanced supply voltages and
c. perturbation of switching angles [8].

Among these imperfections unbalanced supply voltage is of special interest. Converters using four different types of switching functions

are compared in this work. Their performances are studied for both balanced and unbalanced power supply conditions.

In the analysis of converters using different types of switching functions, the input and output currents and output voltages are determined by a method of exact analysis [12].

1.2 Switching Functions

Four switching function schemes are considered and these are:

1. Phase angle controlled switching function
2. Modified sinusoidal PWM switching function
3. PWM switching function for optimum input current distortion and
4. PWM Switching function for specific input current harmonics elimination.

Although many different switching schemes were proposed in past years for conventional six switch converter structure [10,11,13-16], the above mentioned four schemes exhibits better utilisation as compared to others.

1.3 Basis of Comparison

The order and magnitude of harmonic components present in a waveform dictates the size of a filter. Larger filter components calls for greater cost and weight. Relatively larger size filter is required to suppress lower order harmonics in comparison to higher order harmonics. In a 3-phase AC supply system the most consideration is given to reduce

the distortion factor of the input line current. Considering a general second order filter distortion factor can be expressed as [17]

$$DF\% = \frac{[\sum_{n=2}^{\infty} (X_n/n^2)^2]^{\frac{1}{2}}}{X_1} \times 100$$

where:

X_1 = RMS value of the fundamental

X_n = RMS value of the nth harmonic component

The presence of harmonics in a waveform can also be expressed in terms of Total Harmonic Distortion (THD). THD is a measure of the closeness between the waveform and its fundamental component. THD can be expressed mathematically as [17]

$$THD\% = [\sum_{n=2}^{\infty} (X_n/X_1)^2]^{\frac{1}{2}} \times 100$$

where:

X_1 = RMS value of the fundamental

X_n = RMS value of the nth harmonic component

Converters using different switching schemes are compared on the basis of their input power factor, distortion factors of input line current and THD of output voltages for different normalised output dc voltages. Normalised output dc voltage of a AC-DC converter is the

ratio between output dc voltage and it's maximum value. The comparative study is done for balanced and unbalanced supply conditions to establish the performance degradation of different converter schemes under unbalanced supply condition.

The switches are considered ideal and lossless throughout the study.

CHAPTER 2

METHOD FOR ANALYSIS OF 3-PHASE AC-DC CONVERTERS

2.1 Introduction

Fig. 2.1 shows a 3-phase AC-DC converter with six fully-controlled switches. The conduction of individual switch determines the mode of operation. The free-wheeling mode can be achieved by gating two switches on the same arm whenever it is necessary. The input line current, output current and output voltage of a 3-phase AC-DC converter can be determined by solving the differential equations which describes each mode of operation. The different modes of operations are the segments of the whole cycle within which time particular switches conducts and thereby load current is reflected into the line through these particular switches. The solution of these differential equation describing different modes of operation requires much more complicated steps in determining average and effective values because of the presence of mathematically discontinuous voltage and current wave functions. On the other hand the exact method [12] replaces the switches with their proper switching function. This switching function acts like transfer function between input and output. Exact method determines all the input and output quantities in terms of their Fouries series components. In determining input line current, this method handles the output current ripples easily.

In the subsequent analysis the following assumptions have been made.

(i) Continuous load current

(ii) Lossless ideal switches

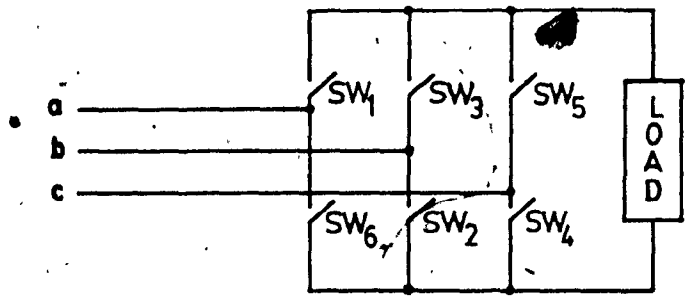

Fig. 2.1 Fully-controlled 3-phase AC-DC converter

(iii) Switches get their timing reference for gating from their respective phases

(iv) Switching functions are symmetrical about origin and have quarter wave symmetry.

2.2 Output Voltage

The transfer function of a converter, $S(\theta)$ can be expressed in terms of its Fourier Series as,

$$S(\theta) = H_n \sin(n\theta + \psi_n) \tag{2.1}$$

Assuming $S_1(\theta)$, $S_2(\theta)$, $S_3(\theta)$, ..., $S_6(\theta)$ as the corresponding gating functions as applied to each switch, the transfer function with respect to port 'a' (Fig. 2.1) becomes $[S_1(\theta) - S_6(\theta)]$.

Similarly the transfer functions for other two input ports are $[S_3(\theta) - S_2(\theta)]$ and $[S_5(\theta) - S_4(\theta)]$ respectively. Assuming the supply phase voltages as:

$$v_a = E_1 \sin(\theta - \phi_1)$$

$$v_b = E_2 \sin(\theta - \phi_2)$$

$$v_c = E_3 \sin(\theta - \phi_3)$$

the output voltage expression becomes

$$v_0(\theta) = \{v_i(\theta)\}\{S(\theta)\} \tag{2.2}$$

or $$v_0(\theta) = F_1(\theta) + F_2(\theta) + F_3(\theta) \qquad (2.3)$$

where:

$v_i(\theta)$ = Input voltage function

$F_1(\theta) = [S_1(\theta) - S_6(\theta)]\, E_1 \sin(\theta - \phi_1)$

$F_2(\theta) = [S_3(\theta) - S_2(\theta)]\, E_2 \sin(\theta - \phi_2)$

$F_3(\theta) = [S_5(\theta) - S_4(\theta)]\, E_3 \sin(\theta - \phi_3)$

By using simple trigonometrical identities and selecting proper terms from output voltage expression, average output voltage becomes

$$V_{dc} = \tfrac{1}{2}(E_1+E_2+E_3)H_1 \cos\alpha \qquad (2.4)$$

Following the same procedure the mth harmonic component of the output voltage can be expressed as

$$\begin{aligned} v_{om} = {} & \frac{E_1 H_{m+1}}{2} \cos\{m\theta - m\phi_1 - (m+1)\alpha\} - \frac{E_1 H_{m-1}}{2} \cos\{m\theta - m\phi_1 - (m-1)\alpha\} \\ & + \frac{E_2 H_{m+1}}{2} \cos\{m\theta - m\phi_2 - (m+1)\alpha\} - \frac{E_2 H_{m-1}}{2} \cos\{m\theta - m\phi_2 - (m-1)\alpha\} \\ & + \frac{E_3 H_{m+1}}{2} \cos\{m\theta - m\phi_3 - (m+1)\alpha\} - \frac{E_3 H_{m-1}}{2} \cos\{m\theta - m\phi_3 - (m-1)\alpha\} \end{aligned} \qquad (2.5)$$

The details of the derivation is shown in Appendix A.

2.3 Output Current

Load impedance to the mth voltage harmonic component is

$$Z_m \angle \delta_m = \{R^2 + (2m\pi fL)^2\}^{\frac{1}{2}} \angle \tan^{-1}\left(\frac{2m\pi fL}{R}\right)$$

Output average current, $I_{dc} = \frac{V_{dc}}{R} - \frac{E_c}{R}$

Considering a specific voltage harmonic component and its corresponding impedance term, the harmonic components of output current can be evaluated. After combining all harmonic components, the output current of the converter can be expressed as

$$i_0(\theta) = I_{dc} + \sum_{n=1}^{\infty} I_n \sin(n\theta + \beta_n) \qquad (2.6)$$

2.4 Input Line Current

Assuming no losses in the converter, input instantaneous power is equal to the output instantaneous power.

$$\{v_i(\theta)\}\{i_i(\theta)\} = \{v_0(\theta)\}\{i_0(\theta)\} \qquad (2.7)$$

From Eqn. 2.2 $v_0(\theta)$ can be expressed in terms of input voltage.

i.e., $\{v_i(\theta)\}\{i_i(\theta)\} = \{v_i(\theta)\}\{S(\theta)\}\{i_0(\theta)\}$

or, $i_i(\theta) = \{S(\theta)\}\{i_0(\theta)\}$ (2.8)

i.e., Instantaneous input line current

$$= \left(\begin{matrix}\text{switching function}\\ \text{of the converter}\end{matrix}\right) \times \left(\begin{matrix}\text{Instantaneous}\\ \text{output current}\end{matrix}\right)$$

By using Eqn. 2.8 an expression for kth harmonic component of input line current can be obtained (see Appendix A) as

$$i_{i,k}(\theta) = I_{dc}\, H_k \sin(K\theta + \psi_k)$$

$$+ \sum_{m=1}^{\infty} \frac{H_m I_{k+m}}{2} \cos(K\theta + \beta_{k+m} - \psi_m)$$

$$- \sum_{m=1}^{K-1} \frac{H_m I_{k-m}}{2} \cos(K\theta + \beta_{k-m} + \psi_m)$$

$$+ \sum_{n=1}^{\infty} \frac{H_{n+k} I_n}{2} \cos(-K\theta + \beta_n - \psi_{n+k}) \qquad (2.9)$$

Third term in expression 2.9 contributes from second harmonic component to higher order harmonic components.

CHAPTER 3

SWITCHING SCHEMES

3.1 Introduction

There are many different switching schemes to improve the output voltage waveshape of inverters [10,11,14,18]. The objective of all these schemes were to eliminate or minimize lower order harmonics from the output voltage waveform of the inverter. These schemes with some exceptions can be used in 3-phase AC-DC converter to improve the waveshape of input line current. Because of the converter structure as shown in Fig. 3.1 and freewheeling option of the load current some modifications are required when these inverter PWM switching functions are implemented in a converter.

Based on the criteria of improved utilization factor four types of switching functions are studied.

3.2 Phase Angle Control

The phase angle controlled switching scheme is shown in Fig. 3.2 for zero phase shift. The timing reference for the occurrence of switching function is derived from the zero crossing of respective phase voltage. The switching function is implemented by the switch pair (SW_1,SW_6), (SW_3,SW_2) or (SW_5,SW_4). The positive portion of the function is implemented by one switch and the negative portion is implemented by another switch in the same arm of the bridge. The switching functions for the other arms are phase shifted from each other according to the phase shift between their respective phase voltages.

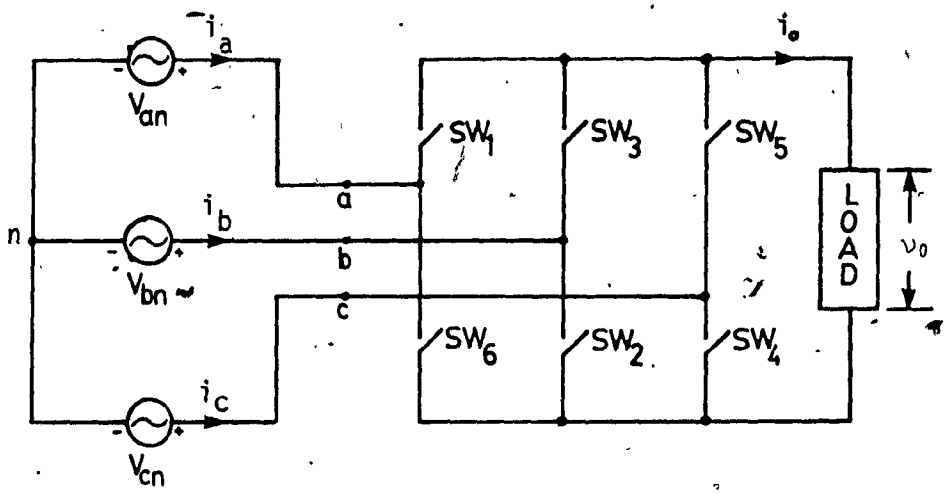

Fig. 3.1 Fully-controlled 3-phase AC-DC converter with input supply.

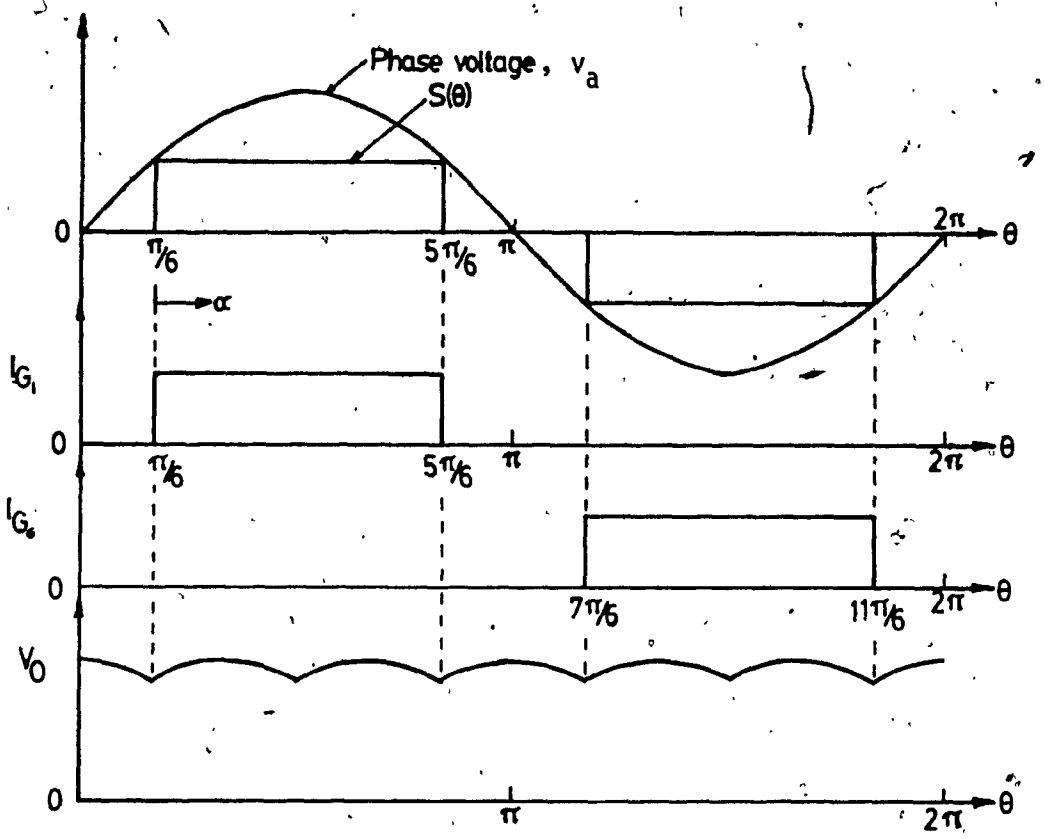

Fig. 3.2 Angle-controlled switching scheme.

For balanced 3-phase supply this phase shift is 120°.

The conduction angle of each individual switch is 120°. This switching function can be delayed by varying the phase shift α to control the average output voltage. Average output voltage depends on the phase shift α and on the fundamental component of the switching function. As the delay increases, displacement power factor of the input line current decreases. Therefore, for lower average output voltage input power factor decreases.

The utilisation factor of an AC-DC converter is expressed as

$$UF = \frac{\text{Maximum output DC voltage}}{\text{RMS input line voltage}} .$$

The utilisation factor for this scheme is, UF = 0.9549.

3.3 Modified Sinusoidal PWM

In modified sinusoidal PWM scheme carrier triangular wave is compared with reference sine wave by leaving middle 60° of the sine wave untouched as shown in Figure 3.3a. The intersections produced from this comparison generates the gating signals for switches. In the gating signals of switch SW_1 the pulses of width D_1, D_2, D_3 and D_4 between π and 2π (as shown in Figure 3.3c) are introduced for freewheeling of load current.

Figure 3.4 shows the positive half of the modified sinuosidal PWM switching function with 12 pulses per half cycle. The switching angles T_1 through T_6 can be derived from intersection points as shown in Figure 3.3a. The remaining switching angles T_7 through T_{12} are derived as follows:

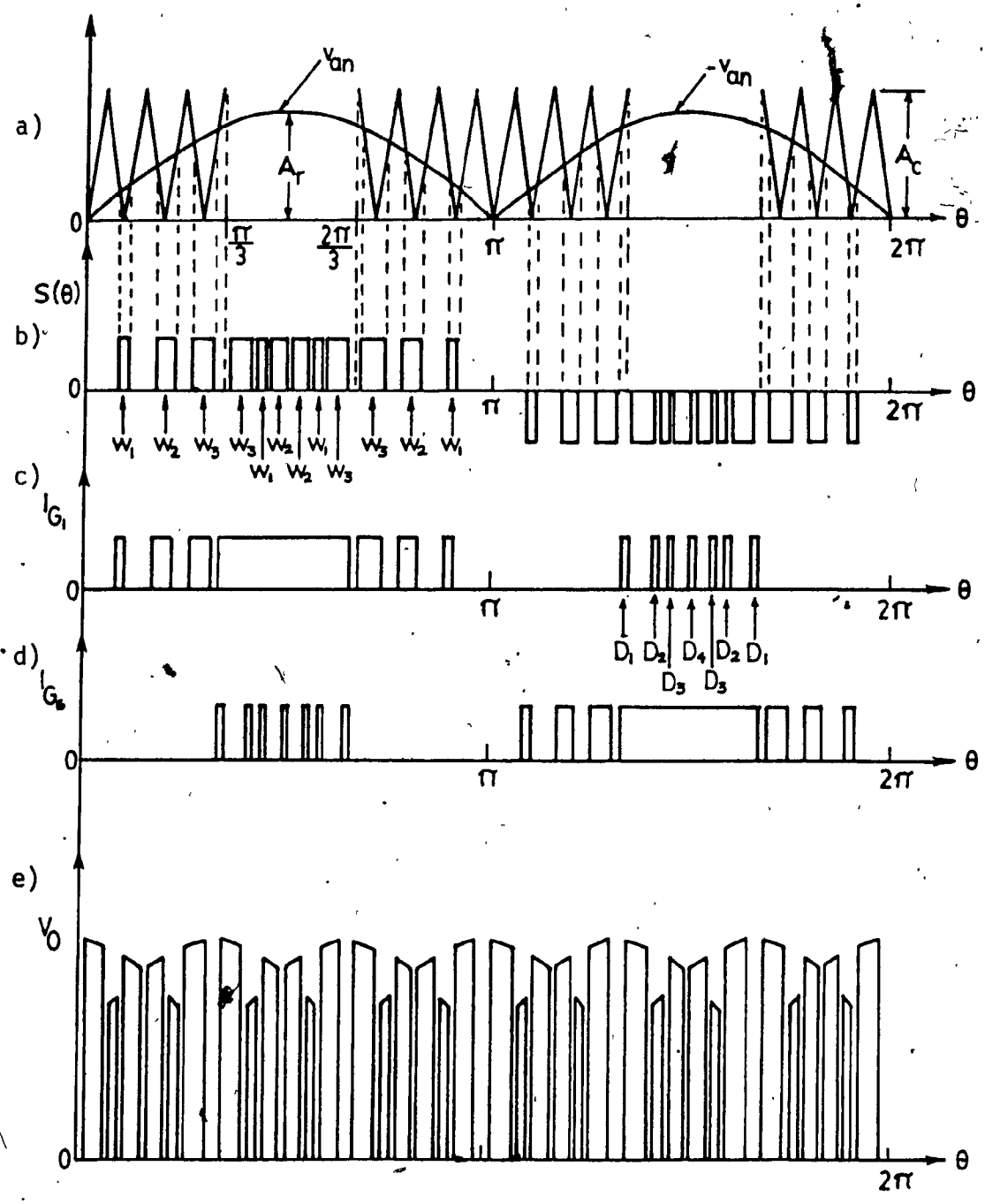

Fig. 3.3 Modified sinusoidal PWM switching scheme.

$$T_7 = \frac{2\pi}{3} - T_6$$

$$T_8 = \frac{2\pi}{3} - T_5$$

$$T_9 = \frac{\pi}{3} + T_1 \qquad (3.1)$$

$$T_{10} = \frac{\pi}{3} + T_2$$

$$T_{11} = \frac{2\pi}{3} - T_4$$

$$T_{12} = \frac{2\pi}{3} - T_3$$

Since the switching function has quarter wave symmetry other angles between $\pi/2$ and π can be derived easily. The number of pulses per half cycle in the switching function can be increased by varying normalised carrier frequency. The width of pulses are varied by varying modulation index, where modulation index is expressed as

$$M = \frac{A_r}{A_c}$$

The output voltage can be varied by changing the modulation index.

The pulse width D_1, D_2, D_3 and D_4 in the gating signal in Figure 3.3 can be obtained from the geometry of Figure 3.3a and Figure 3.4. These are as follows:

$$D_1 = \frac{\pi}{3} - T_6$$

$$D_2 = T_1 + T_5 - \frac{\pi}{3} \qquad (3.2)$$

$$D_3 = \frac{\pi}{3} - T_2 - T_4$$

$$D_4 = 2T_3 - \frac{\pi}{3}$$

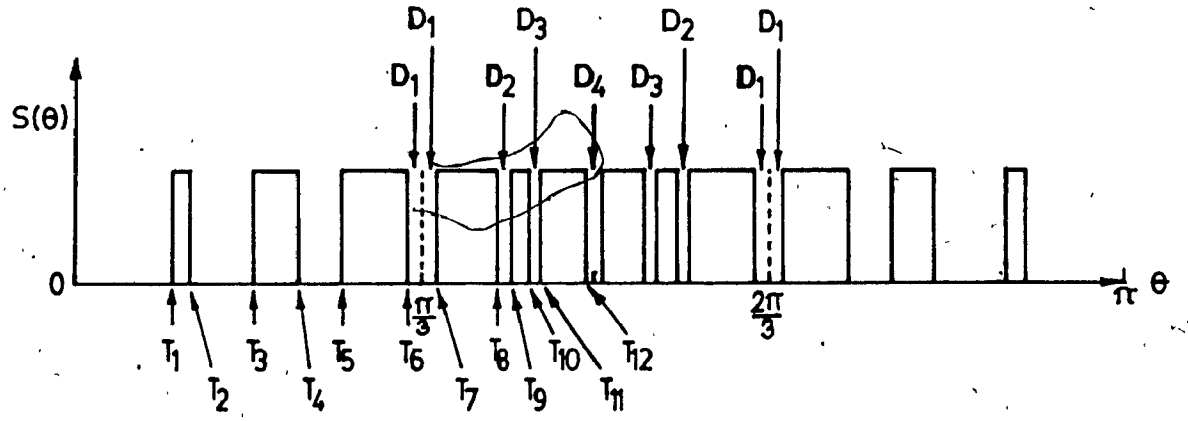

Fig. 3.4 Modified sinusoidal PWM switching function, 12 pulses per half cycle.

The dominant harmonic component of the input line current is shifted toward higher order frequency with the increase in the number of pulses per half cycle. Therefore the distortion factor of input line current decreases with the increase of pulses. Since the switching function does not require any phase shift for output voltage variation, the displacement power factor can be maintained at unity throughout the voltage range.

The number of pulses per half cycle of this switching scheme is $N_p = 4P$, where P is the number of pulses within 0°-60°. The ratio of the carrier frequency f_c to the input supply frequency f_i can be expressed as

$$\frac{f_c}{f_i} = 6m + 3 \qquad (3.3)$$

where m is an integer.

The utilisation factor for this scheme is,

UF = 0.8631, for 12 pulses/half cycle

and UF = 0.8643, for 16 pulses/half cycle.

3.4 Optimum Distortion Factor

A fixed PWM switching function can be obtained by varying the width of the pulses by trial and error until the distortion factor of the input line current is minimized. Theoretically, an infinite number of pulses would be required to bring this distortion factor down to zero. However, in practice, the pulse number is limited by the factors of switching loss and insignificant improvement of distortion factor after a certain

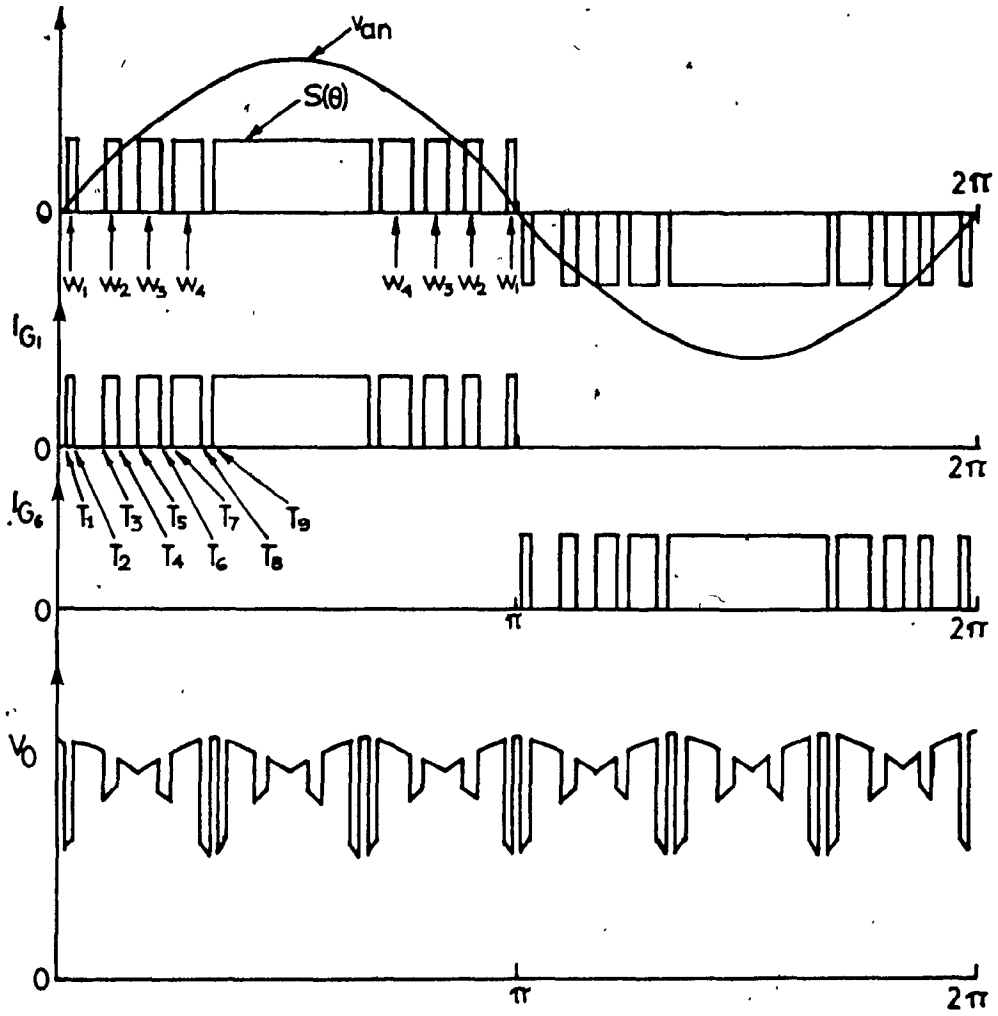

Fig. 3.5 PWM switching scheme for optimum input current distortion.

pulse number.

Figure 3.5 shows a PWM switching function for optimum distortion factor having 9 pulses per half cycle and also having quarter wave symmetry. To satisfy the continuous load current condition, the switching function should also meet some criterion in terms of its pulse width as shown in Figure 3.6. Once the switching function is constrained to this condition, the distortion factor becomes the function of switching angles as follows:

$$DF = f(T_1, T_2, T_3, \ldots, T_n) \tag{3.4}$$

where number of pulses per half cycle becomes (2n+1).

A suitable algorithm can be used for Eqn. 3.4 to determine the switching angles T_1 through T_n for optimum distortion factor (see Appendix B). The remaining switching angles are derived by satisfying the pulse-width condition as shown in Figure 3.6. For a switching function of 9 pulses per half cycles, switching angles T_1 through T_4 are derived by optimising DF in Eqn. 3.4. The remaining switching angles within 90° are derived as follows.

$$\begin{aligned} T_5 &= \frac{\pi}{6} \\ T_6 &= \frac{\pi}{3} - T_4 \\ T_7 &= \frac{\pi}{3} - T_3 \\ T_8 &= \frac{\pi}{3} - T_2 \\ T_9 &= \frac{\pi}{3} - T_1 \end{aligned} \tag{3.5}$$

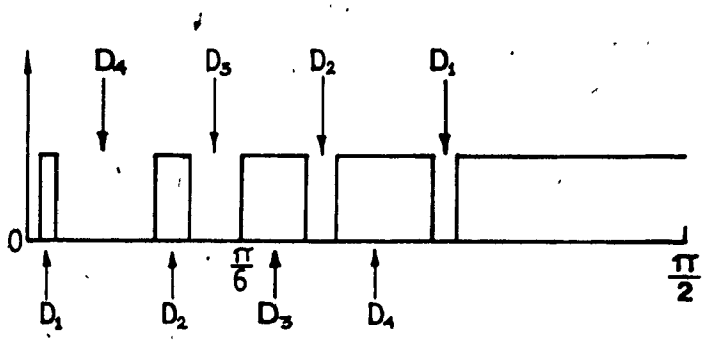

Fig. 3.6 PWM switching function for optimum input current distortion.

The optimum distortion factor decreases with the increase of pulses in the switching function. The output voltage can be varied by phase shifting the switching function.

Some switching functions which produces optimum distortion in the input line current of the converter are illustrated in Figs. 3.7, 3.8 and 3.9. Only a quarter cycle of the wave is shown for the sake of convenience.

The utilisation factor for this scheme is,

UF = 0.8874, for 9 pulses per half cycle

and UF = 0.8839, for 11 pulses per half cycle.

3.5 Specific Harmonic Elimination

Specific harmonic components of input line current can be eliminated by introducing a suitable PWM switching function. Basically the scheme is identical to the scheme for optimum distortion as described in Section 3.4 except the way the switching angles are derived. For specific harmonics elimination, switching angles are derived from the expressions of specific harmonic component terms which are constrained to zero. A set of nonlinear equations is derived (see Appendix C). The specific harmonic term is

$$H_m = f(T_1, T_2, T_3, \ldots, T_n) = 0 \qquad (3.6)$$

where m is the order of harmonic component.

The number of equations to be solved is equal to the number of specific harmonics to be eliminated, which again is equal to n. The

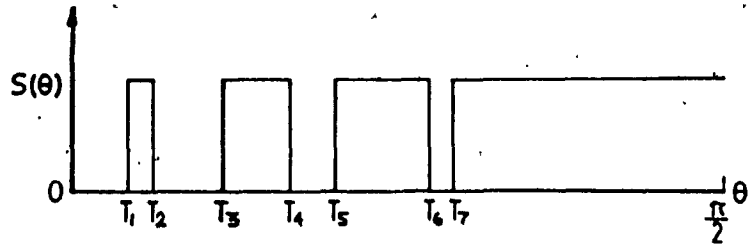

Fig. 3.7 PWM switching function for optimum input current distortion, 7 pulses per half cycle.
T_1=7.4°, T_2=10.9°, T_3=22.9°, T_4=30°,
T_5=37.1°, T_6= 49.1°, T_7=52.6°, DF=.117%

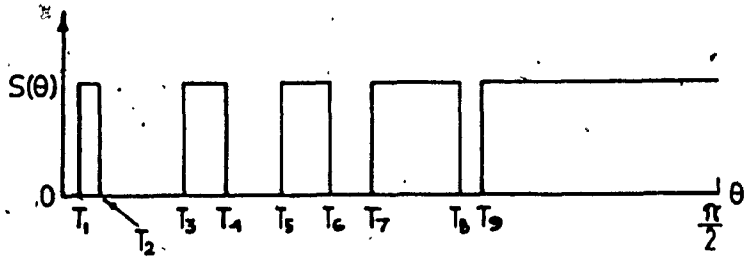

Fig. 3.8 PWM switching function for optimum input current distortion, 9 pulses per half cycle.
T_1=2°, T_2=4.6°, T_3=17.4°, T_4=22.3°,
T_5=30°, T_6=37.7°, T_7=42.6°, T_8=55.4°
T_9=58°, DF=.0765%

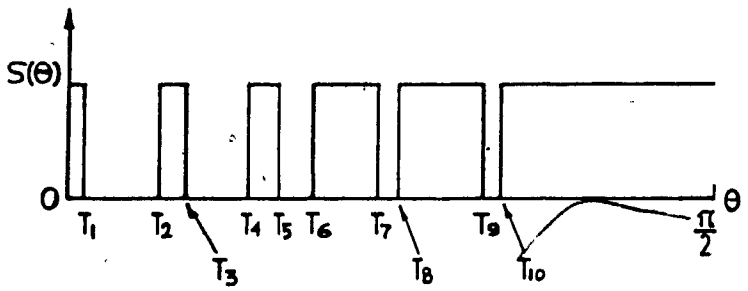

Fig. 3.9 PWM switching function for optimum input current distortion, 11 pulses per half cycle. T_1=2.1°, T_2=13.8°, T_3=17.3°, T_4=24.8°, T_5=30°, T_6=35.2°, T_7=42.7°, T_8=46.2°, T_9=57.9°, T_{10}=60°, DF=.052%

switching angles T_1 through T_n are derived by solving the set of nonlinear Equations 3.6. The remaining switching angles are derived by satisfying virtual symmetry about 30° similar as shown in Figure 3.6 in Section 3.3. The number of pulses per half cycle is (2n+1).

To obtain a possible lower value of distortion factor, lower order harmonic components are eliminated. For 3 pulses per half cycle, 5th and 7th harmonic components can be eliminated. Switching angles for 5 and 7 pulses per half cycle are shown in Figure 3.10 and 3.11. A proper solution for 9 pulses per half cycle in order to eliminate 5,7,11 and 13th harmonic components with the required constraints is nonexistent. A solution with more than 9 pulses per half cycle was not tested.

The utilisation factor for this scheme is UF = 0.8914, for 5 pulses per half cycle and UF = 0.8833, for 7 pulses per half cycle.

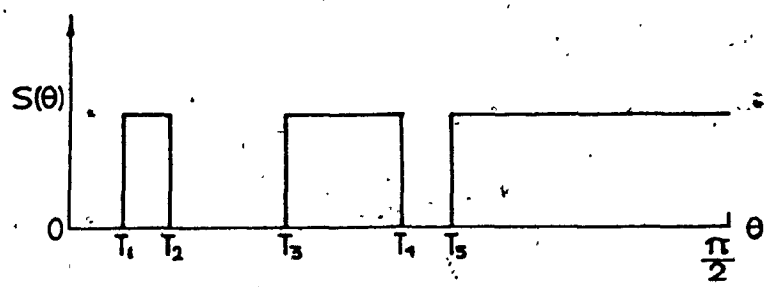

Fig. 3.10 PWM switching function for specific harmonic elimination, 5 pulses per half cycle. T_1=7.93°, T_2=13.75°, T_3=30°, T_4=46.25°, T_5=52.07°

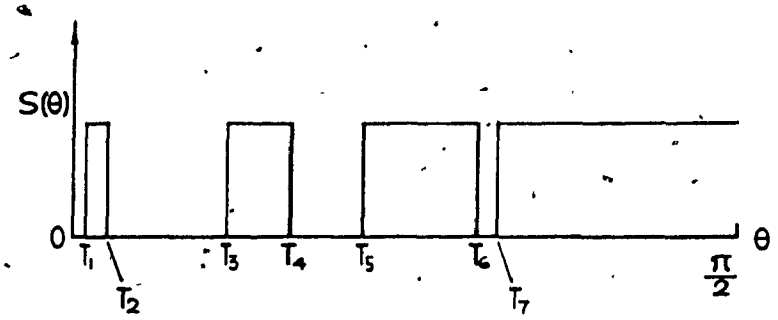

Fig. 3.11 PWM switching function for specific harmonic elimination, 7 pulses per half cycle. T_1=2.24°, T_2=5.6°, T_3=21.26, T_4=30°, T_5=38.74°, T_6=54.4°, T_7=57.76°.

CHAPTER 4

COMPARISON BETWEEN DIFFERENT SWITCHING SCHEMES

4.1 Introduction

Computer programs have been developed for different switching schemes to determine the utilisation factor, input power factor, distortion factor of input line current and total harmonic distortion of output voltage. This comparative study is done for balanced and unabalanced supply conditions. It is important to mention here that the modified sinusoidal PWM switching function and the switching function for optimum distortion factor can have different number of pulses. Depending on the value of input line current's distortion factor, 16 pulses per half cycle for modified sinusoidal PWM and 11 pulses per half cycle for optimum distortion factor switching function has been chosen. Because, beyond these pulse numbers any increase in the pulse number does not contribute to decrease the distortion factor significantly. Figure 4.1 shows the variation of input line current's distortion factor with the increase of number of pulses for modified sinusoidal PWM switching function and optimum distortion factor switching function. The curves in Figure 4.1 are drawn for maximum output dc voltage condition.

7 pulses per half cycle has been considered for the switching function to eliminate specific harmonics in input line current. Pulse number beyond 7 is not considered because a proper solution having 9 pulses per half cycle to eliminate 5,7,11 and 13th harmoinc components is nonexistent. The different switching schemes will be denoted by number 1, 2,3 and 4.

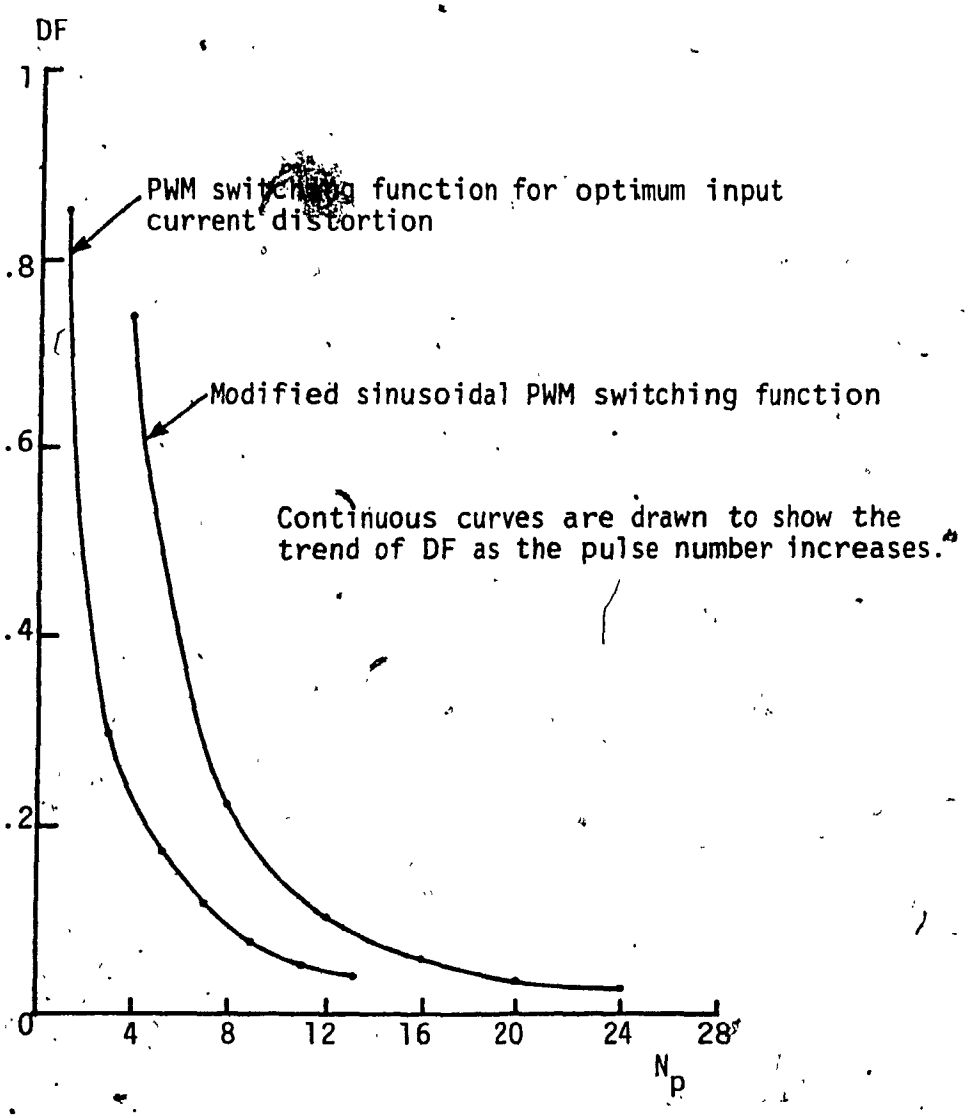

Fig. 4.1 DF versus number of pulses per half cycle.

Phase angle controlled switching function	1
Modified sinusoidal PWM switching function	2
Switching function for optimum input current distortion	3
Switching function for specific input current harmonics elimination	4

4.2 Frequency Spectrum of Switching Functions

Frequency spectrum of a switching function represents the line current of a converter under ripple free load current condition. But in practice the load current of all AC-DC converters contains some ripple. The ripple content in the load current decreases with the increase of load inductance. Because of the presence of ripple in the load current, the frequency spectrum of input line current will deviate from the frequency spectrum of it's switching function. This deviation becomes greater for unbalanced supply voltage.

Figure 4.2 through 4.5 show the frequency spectrum of the switching functions which are considered in this study. Since each supply line conducts 120° in positive half cycle and another 120° in negative half cycle, the effective value of all switching functions are fixed. So a reduction or elimination of lower order harmonics results in increase in relative amplitude of higher order harmonics.

4.3 Utilisation Factor

Utilisation factor denotes the maximum possible output dc voltage converters can produce from same supply. So for the same switches, supply and constant load current, utilisation factor indicates the

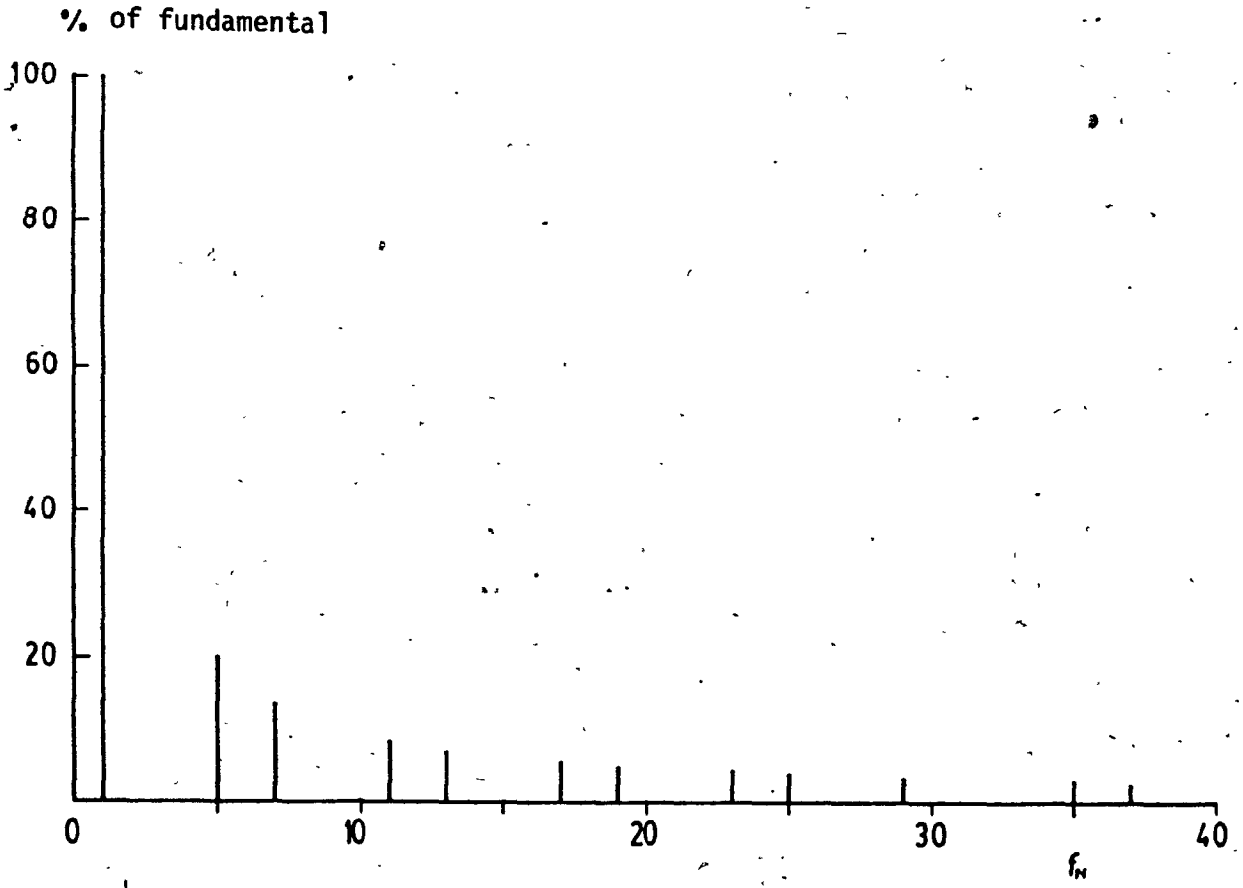

Fig. 4.2 Frequency spectrum of angle-controlled switching function.

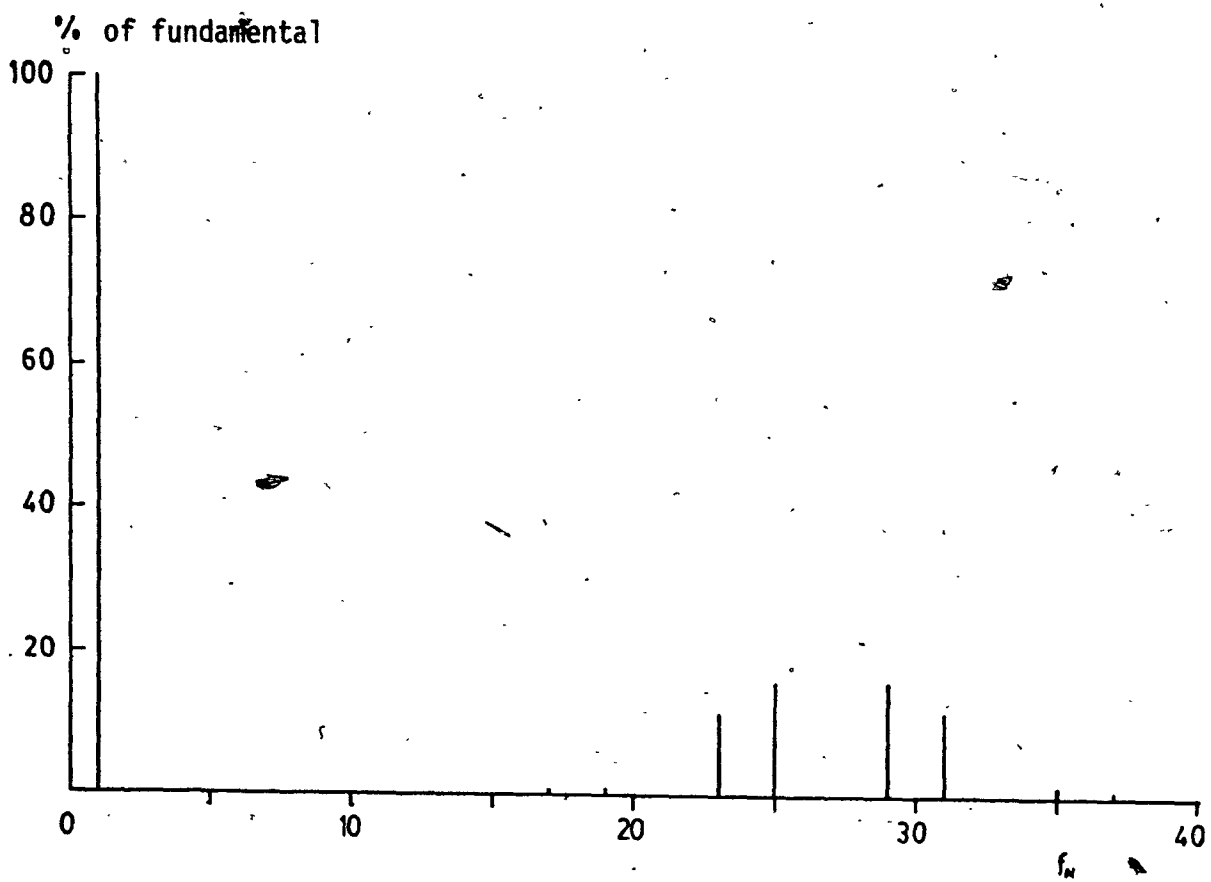

Fig. 4.3 Frequency spectrum of modified sinusoidal PWM switching function.

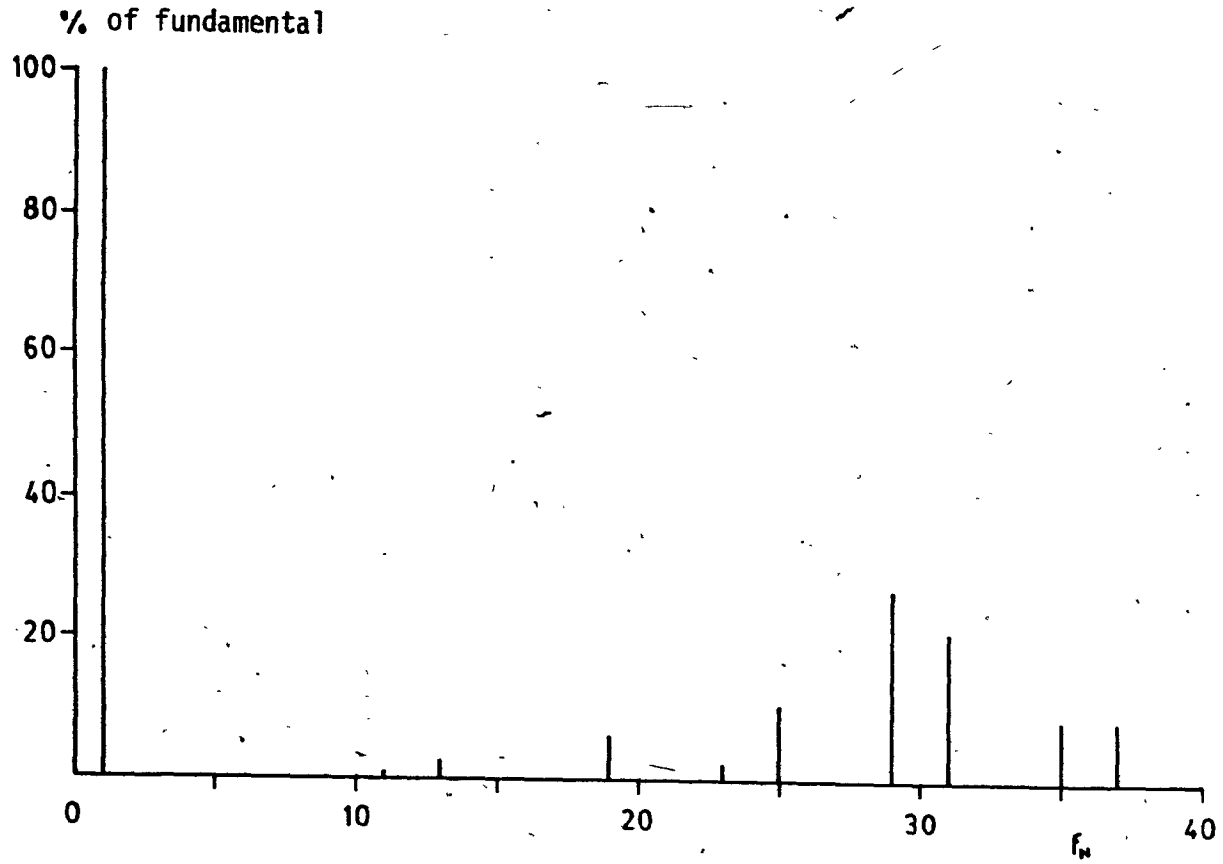

Fig. 4.4 Frequency spectrum of switching function for optimum input current distortion.

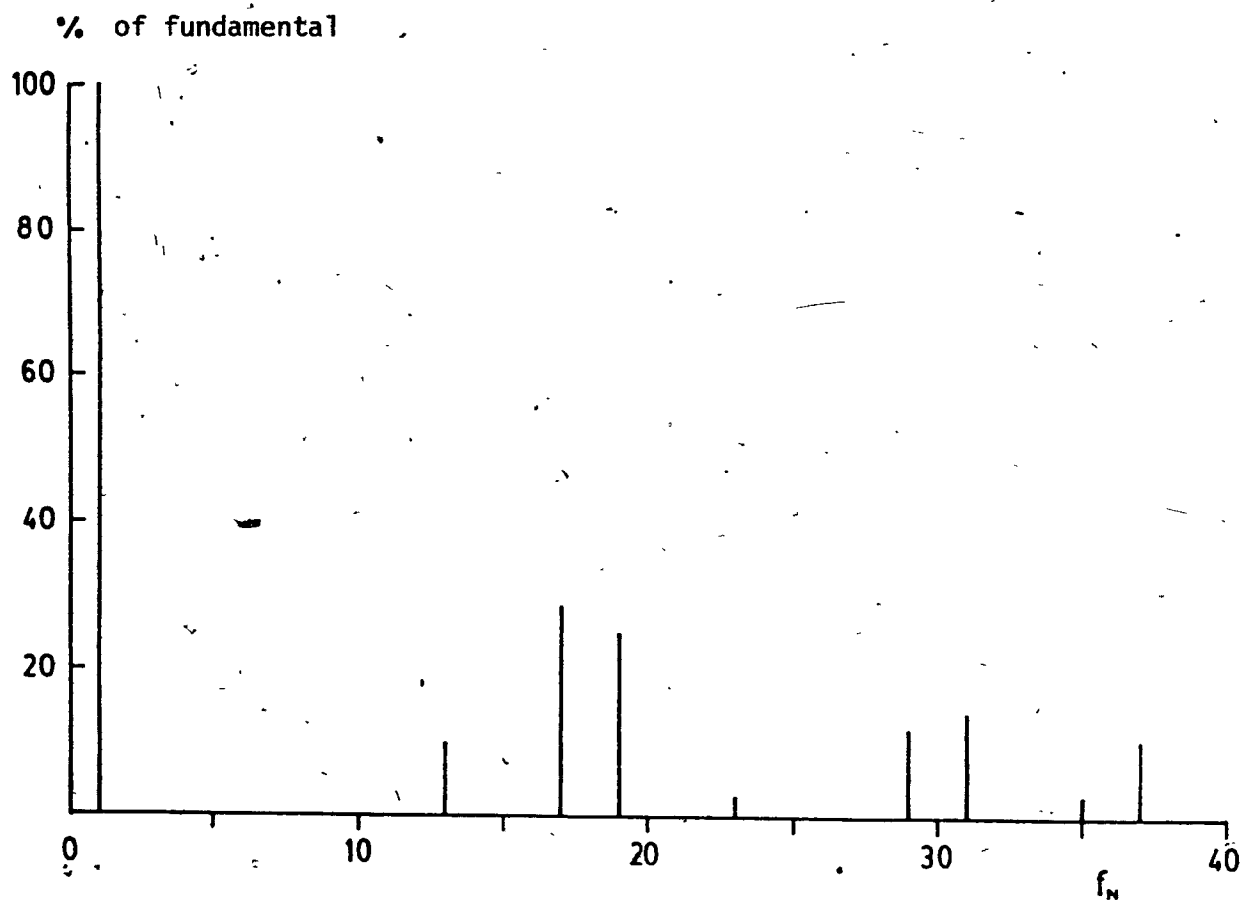

Fig. 4.5 - Frequency spectrum of switching function for specific harmonic elimination.

maximum power conversion capability of the converter.

Table 1 shows the utilisation factor and its normalised value with respect to scheme 1 for different switching schemes. Scheme 4 shows better utilisation for less number of pulses in comparison to scheme 2 and 3. It may be noted that the maximum output dc voltage occurs at $\alpha=0$ for schemes 1,3,4 and at $M=1.0$ for scheme 2.

TABLE 1

SCHEMES	UF	N_p	Normalised UF
1	.9549	1	1
2	.8643	16	.9051
3	.8839	11	.9256
4	.8833	7	.9250

4.4 Input Power Factor

Semiconductor switches are passive element. So the converters having semiconductor switches require reactive current. In general the converters can operate at a satisfactory power factor at full load. However, the power factor decreases with the reduction of dc output voltage.

For balanced supply voltage input power factor of a converter can be expressed under the assumption of a series load as [16].

$$PF = \frac{I}{I_i} \cos \gamma_1 \qquad (4.1)$$

where:

I = RMS value of fundamental input current

I_i = RMS value of input current

γ_1 = Phase angle between input fundamental current and corresponding phase voltage

For unbalanced supply voltage or unbalanced load, the concept of average power factor as used in balanced case is no more valid. Average power factor for unbalanced case can be defined as the average of individual phase power factors only when the load is fully inductive or fully capacitive [19].

Fig. 4.6 shows the input power factor of the converter with respect to normalised output dc voltage for balanced supply. Figs. 4.7 and 4.8 shows the input power factor for unbalanced supply. Two unbalanced cases are considered for comparative study. They are as follows:

CASE 1

$V_{ab} = 1.546 \underline{/-27.18°}$, $V_{bc} = 1.432 \underline{/80.06°}$

and $V_{ca} = 1.769 \underline{/-156.54°}$

CASE 2

$V_{ab} = 1.662 \underline{/-27.33°}$, $V_{bc} = 1.527 \underline{/88.29°}$

and $V_{ca} = 1.703 \underline{/-153.38°}$

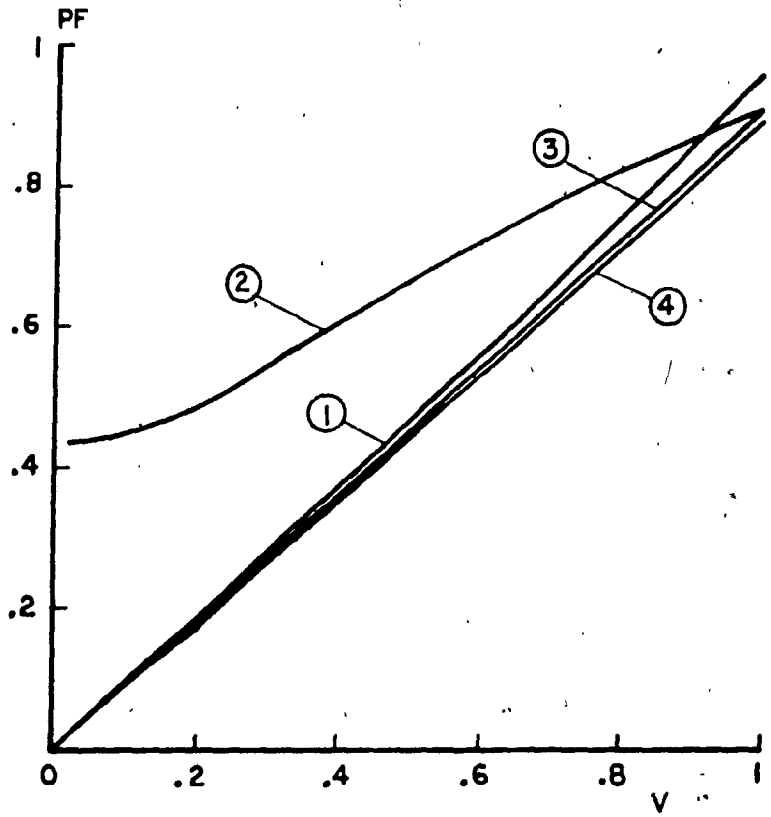

Fig. 4.6 Power factor of different schemes. (Balanced supply)

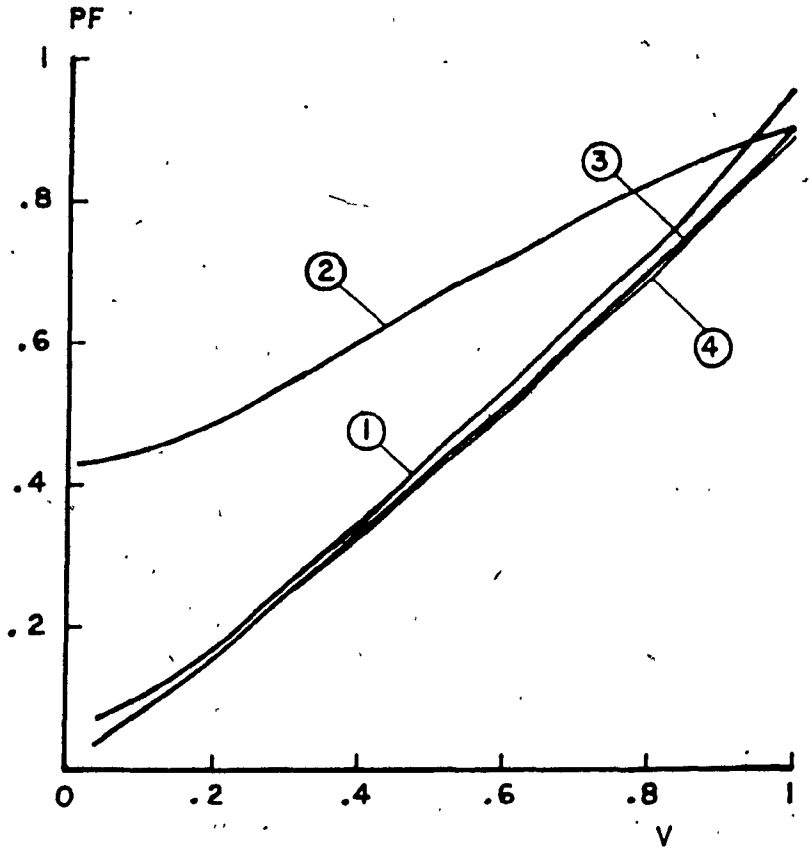

Fig. 4.7 Power factor of different schemes. (Unbalanced supply. $V_{ab} = 1.546/\underline{-27.18°}$, $V_{bc} = 1.432/\underline{80.06°}$, $V_{ca} = 1.769/\underline{-156.54°}$).

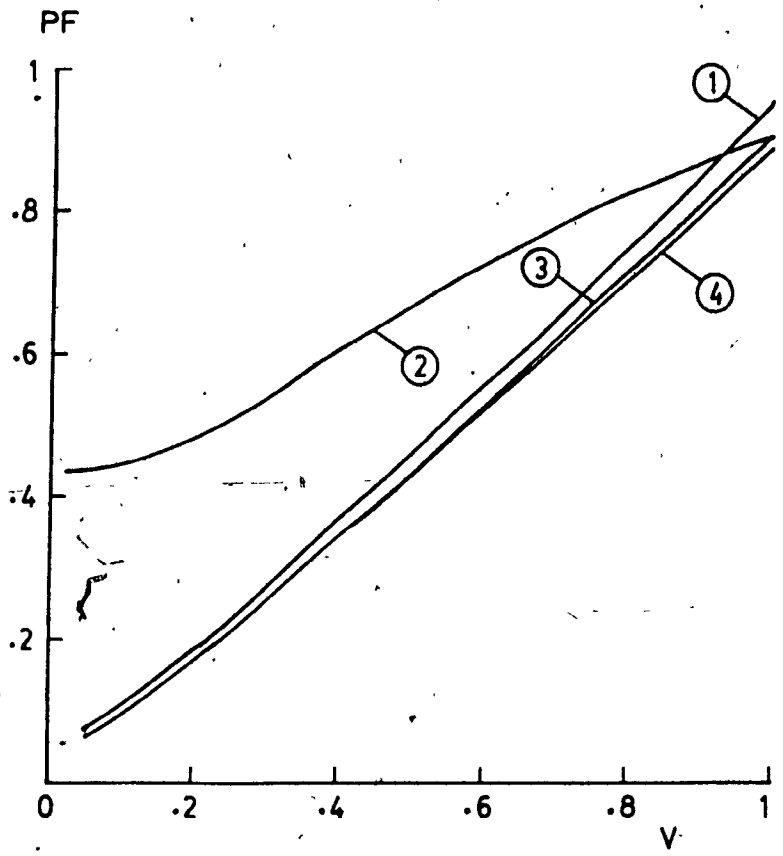

Fig. 4.8 Power factor of different schemes. (Unbalanced supply. $V_{ab} = 1.662\underline{/-27.33°}$, $V_{bc} = 1.527\underline{/88.29°}$, $V_{ca} = 1.703\underline{/-153.38°}$).

All voltages are expressed in per unit. The selection of these unbalanced line voltages are shown in Appendix D.

The power factor of scheme 2 is better than all other schemes both for balanced and unbalanced supply conditions, until the normalised dc output voltage become approximately 0.9. When the normalised output dc voltage is increased beyond 0.9, scheme 1 exhibits better power factor in comparison to others for balanced as well as unbalanced supply condition. Although scheme 3 shows better power factor than scheme 4, the difference is insignificant for balanced and unbalanced supply cases.

4.5 Distortion Factor

The input power factor and the distortion factor are the two important parameters from supply point of view regarding converter performances. The prsence of harmonic components in the system line current produces increased losses in all system components and creates malfunctioning of shopisticated electrical and electronic equipments. The distortion factor represents the presence of lower order harmonics at the converter input. A generalised second order filter is considered to evaluate the distortion factors of all four schemes.

Figs. 4.9 and 4.10 show the distortion factor for different normalised output dc voltage under balanced supply condition. The distortion factors of scheme 2,3 and 4 are considerably smaller in comparison to scheme 1.

Figs. 4.11 and 4.12 show the distortion factor under unbalanced supply condition. The distortion factor of scheme 2 is smallest in comparison to other schemes for unbalanced supply. In general the distortion

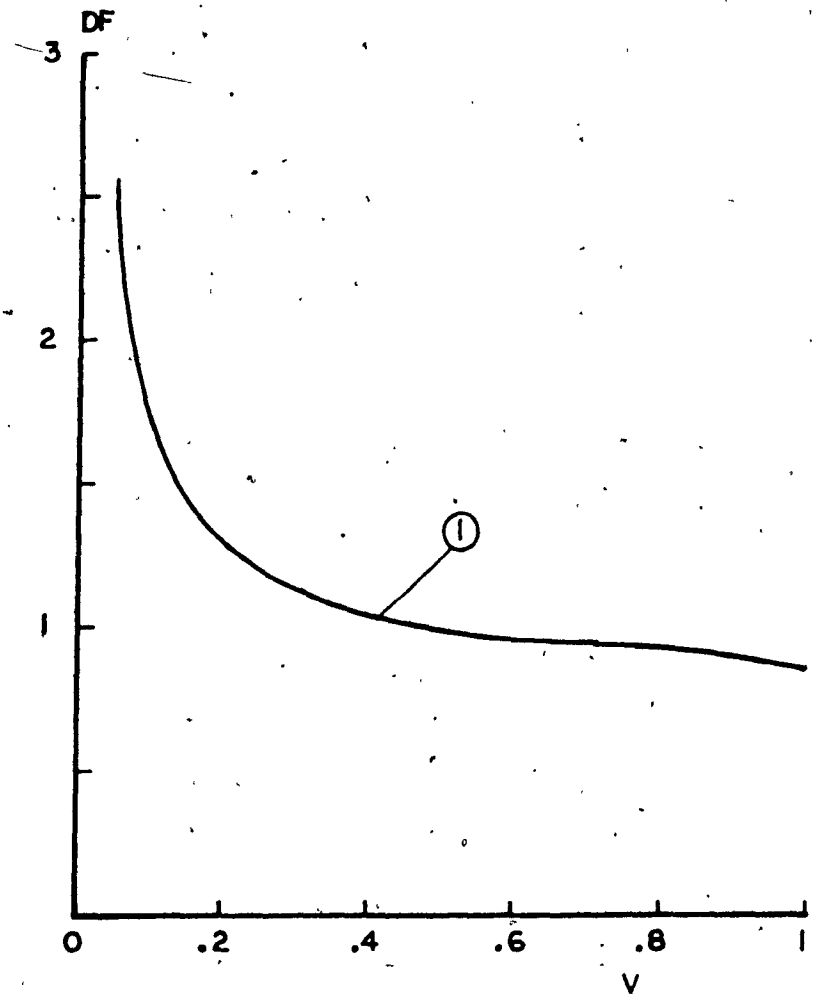

Fig. 4.9 Distortion factor of scheme 1 (Balanced supply).

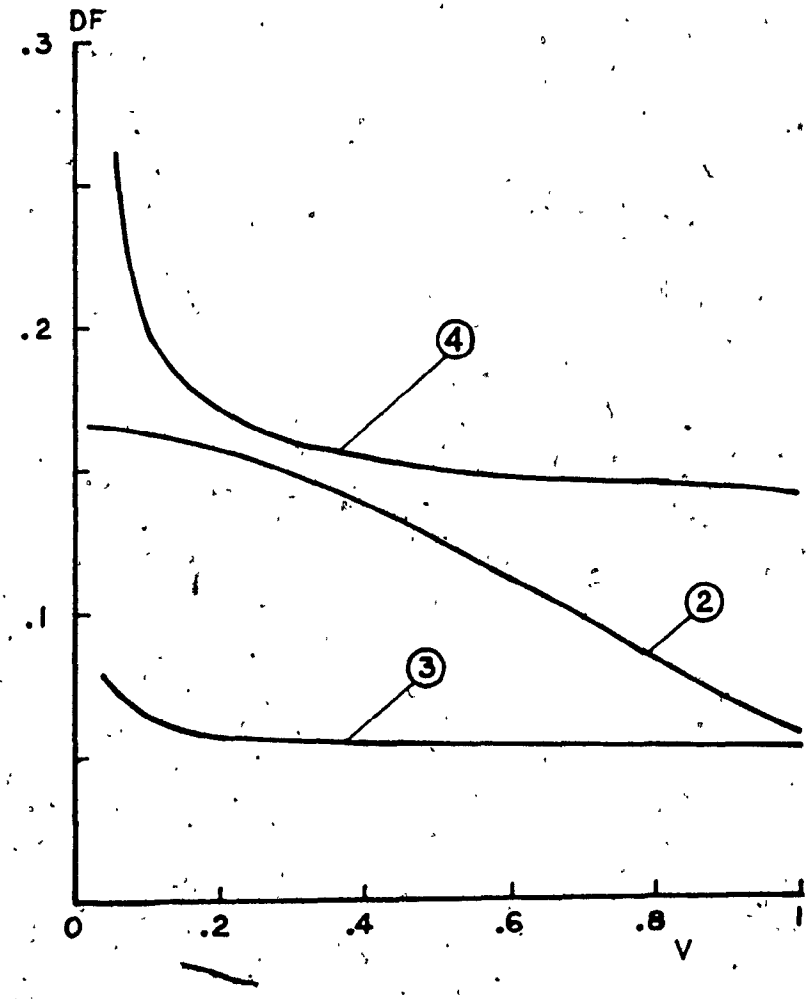

Fig. 4.10 Distortion factor of different schemes. (Balanced supply)

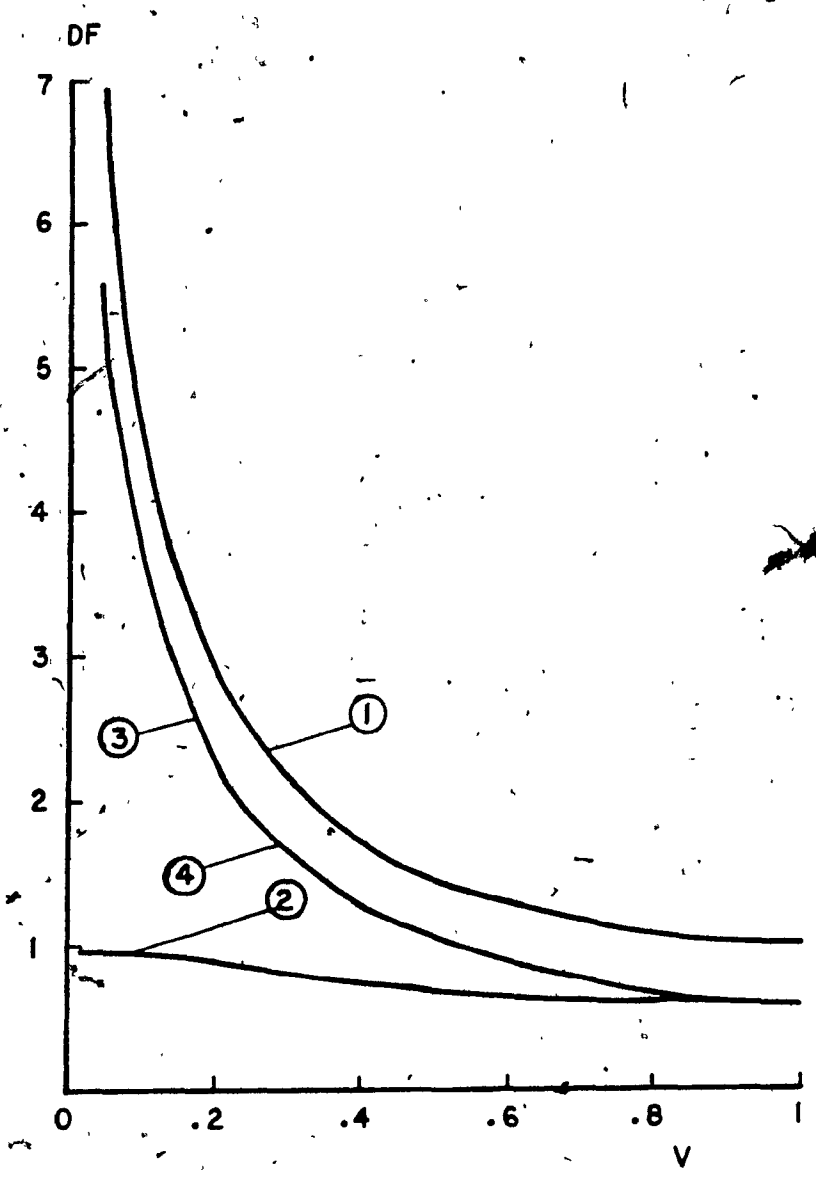

Fig. 4.11 Distortion factor of different schemes.
(Unbalanced supply. $V_{ab} = 1.546/\underline{-27.18°}$,
$V_{bc} = 1.432/\underline{80.06°}$, $V_{ca} = 1.769/\underline{-156.54°}$)

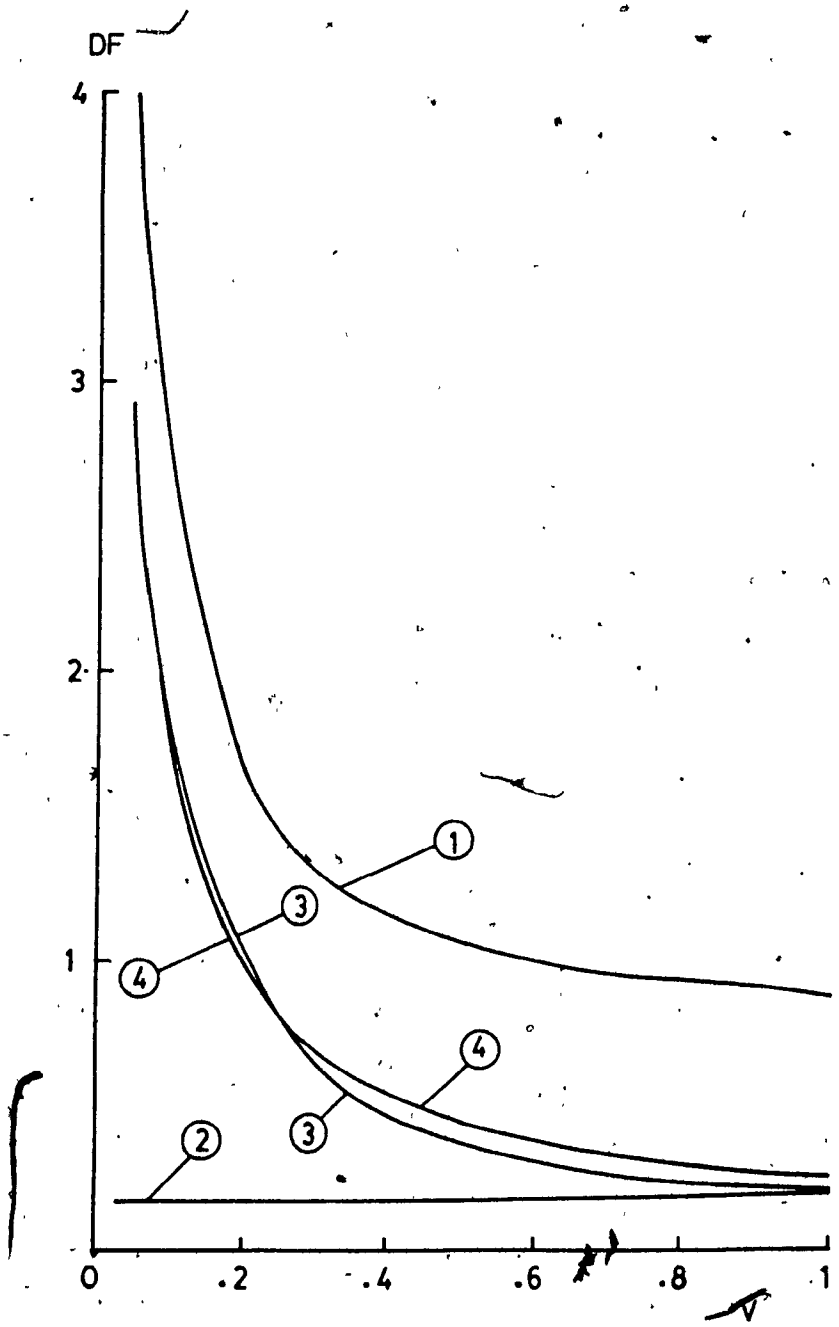

Fig. 4.12 Distortion factor of different schemes.
(Unbalanced supply. $V_{ab} = 1.662/\underline{-27.33°}$,
$V_{bc} = 1.527/\underline{88.29°}$, $V_{ca} = 1.703/\underline{-153.38°}$)

factor of all schemes is deteriorated when the supply becomes unbalanced.

4.6 THD of Output Voltage

The total harmonic distortion of output voltage is a measure of the closeness of output voltage waveshape to its average value. Higher ripple content make the THD higher. In general all practical load has some inductance. This inductance improves the output current waveshape. So for output filtering the load inductance gives added advantage.

Fig. 4.13 shows the THD with respect to normalised output dc voltage for balanced supply. Figs. 4.14 and 4.15 show THD for unbalanced supply. For both balanced and unbalanced supply conditions, scheme 1 exhibits better output voltage THD for most of the output dc voltage range. The output voltage THD of scheme 3 and 4 are very close to each other for both balanced and unbalanced supply conditions.

Although THD gives an idea about waveshape, it does not give a clear indication about output filtering requirement. The frequency spectrum of output voltage gives a clear picture about output filtering requirement. Table 2 shows the frequency spectrum of output voltage under balanced supply condition. Table 3 and Table 4 show the frequency spectrum of output voltage under unbalanced supply conditions. The order of the dominant harmonic components of schemes 2,3 and 4 are greater than the dominant harmonic component of scheme 1 for balanced supply condition. Under unbalanced supply conditions second harmonic component becomes significant in comparison to other harmonic components.

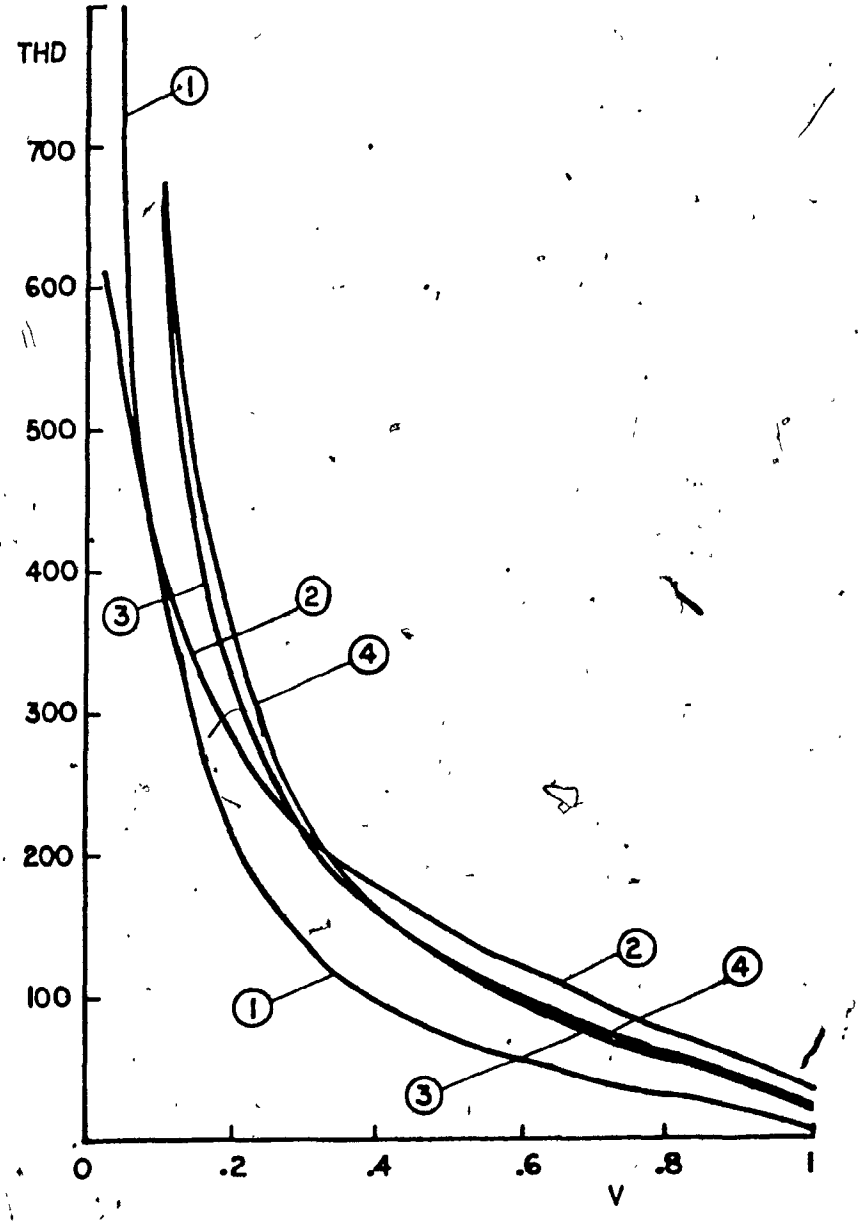

Fig. 4.13 Output voltage THD of different schemes. (Balanced supply)

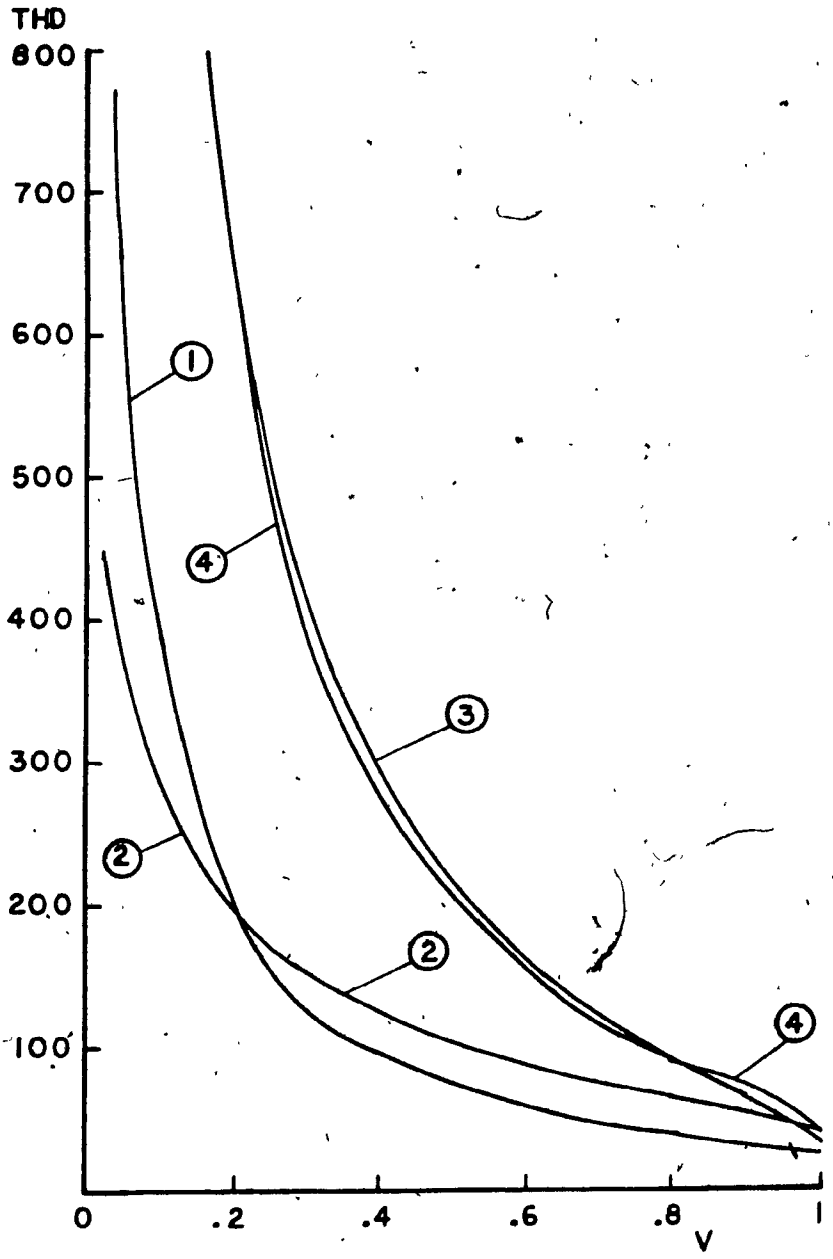

Fig. 4.14 Output voltage THD of different schemes. (Unbalanced supply. $V_{ab} = 1.546/\underline{-27.18°}$, $V_{bc} = 1.432/\underline{80.06°}$, $V_{ca} = 1.769/\underline{-156.54°}$)

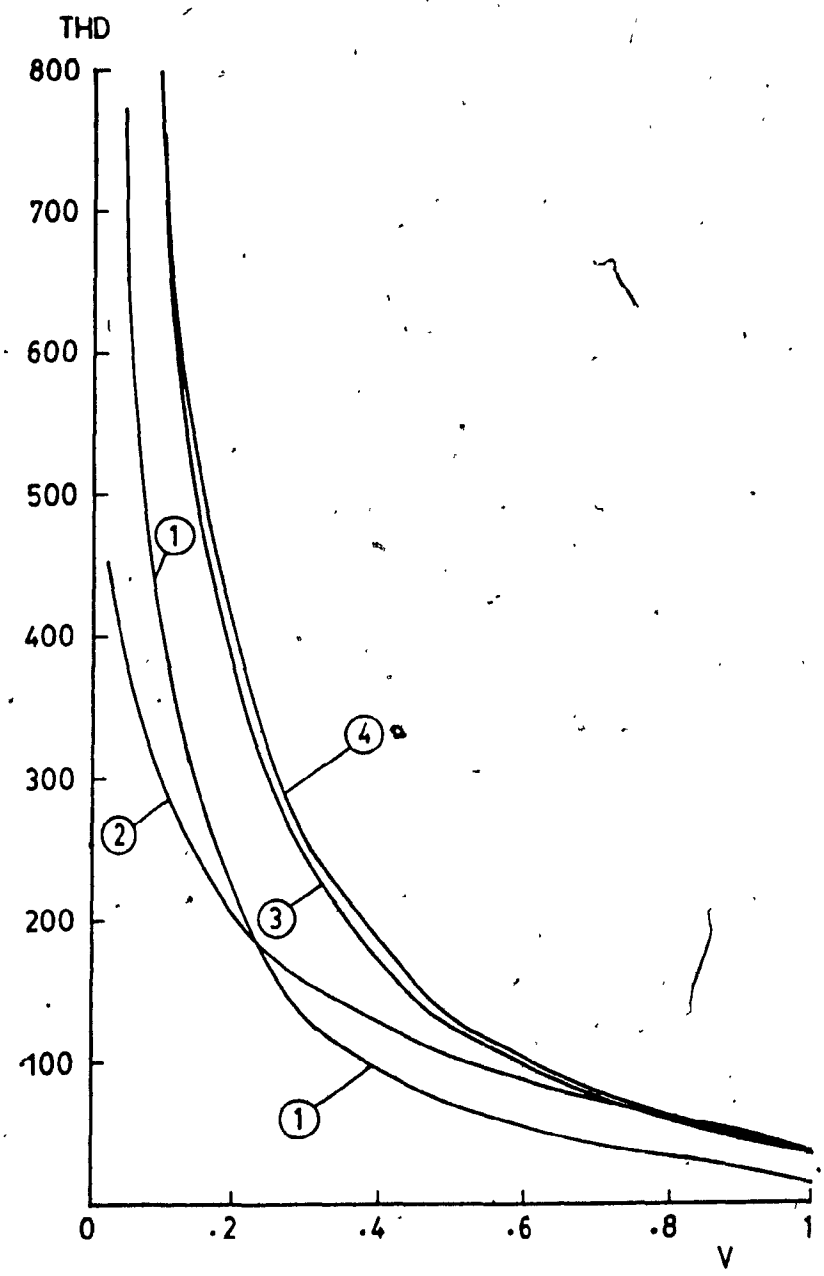

Fig. 4.15 Output voltage THD of different schemes.
(Unbalanced supply. $V_{ab} = 1.662/\underline{-27.33°}$,
$V_{bc} = 1.527/\underline{88.29°}$, $V_{ca} = 1.703/\underline{-153.38°}$)

TABLE 2

FREQUENCY SPECTRUM OF OUTPUT VOLTAGE
AMPLITUDE EXPRESSED AS A PERCENTAGE OF CORRESPONDING AVERAGE VALUE
BALANCED SUPPLY

Harmonic Order n	SCHEME 1		SCHEME 2		SCHEME 3		SCHEME 4	
	V_N=1	V_N=.5	V_N=1	V_N=.5	V_N=1	V_N=.5	V_N=1	V_N=.5
6	5.713	59.661	0.401	1.356	0.549	0.705	0.0	0.026
12	1.397	29.105	0.461	1.919	3.814	4.217	10.555	21.137
18	0.617	19.311	1.082	4.188	6.643	12.415	4.137	94.484
24	0.351	14.462	14.455	66.107	13.161	19.269	2.967	6.98
30	0.224	11.559	14.522	66.389	4.977	83.969	1.889	46.536
36	0.157	9.625	1.369	5.154	0.085	29.478	8.261	25.673
42	0.115	8.259	1.763	4.805	7.583	10.718	8.49	8.523

TABLE 3

FREQUENCY SPECTRUM OF OUTPUT VOLTAGE
AMPLITUDE EXPRESSED AS A PERCENTAGE OF CORRESPONDING AVERAGE VALUE

UNBALANCED SUPPLY, $V_{ab} = 1.546/-27.18°$, $V_{bc} = 1.432/80.06°$,
$V_{ca} = 1.769/-156.54°$

Harmonic Order n	SCHEME 1		SCHEME 2		SCHEME 3		SCHEME 4	
	V_N=1	V_N=.5	V_N=1	V_N=.5	V_N=1	V_N=.5	V_N=1	V_N=.5
2	18.776	37.553	18.773	18.768	18.778	37.557	18.778	37.582
4	4.048	8.095	0.044	0.132	0.028	0.057	0	0
6	4.927	51.468	0.343	1.173	0.471	0.614	0	0.014
8	6.561	13.122	0.095	0.322	0.186	0.371	0	0
10	5.271	10.542	0.124	0.513	0.8	1.6	0.007	0.014
12	0.721	14.96	0.241	0.982	1.957	2.171	5.425	10.873
14	4.114	8.227	0.131	0.557	1.3	2.6	5.647	11.302
16	4.755	9.51	0.299	1.378	0.236	0.471	23.695	47.425
18	0.178	5.675	0.314	1.232	1.95	3.643	1.215	27.739
20	2.229	4.458	0.299	1.056	2.693	5.386	10.672	21.359
22	3.472	6.944	9.072	5.235	2.007	4.014	2.645	5.293
24	0.212	8.757	8.744	39.956	7.964	11.671	1.794	4.22
26	1.091	2.182	7.027	16.202	2.9	5.8	0.093	0.186
28	1.898	3.796	14.207	32.771	14.686	29.371	6.862	13.734
30	0.192	9.894	12.425	56.745	4.257	71.9	1.615	39.843
32	1.111	2.222	3.886	2.317	7.457	14.914	4.932	9.871
34	0.721	1.442	0.212	0.733	2.164	4.328	0.729	1.459
36	0.132	8.294	1.176	4.428	0.071	25.386	7.105	22.117
38	1.243	2.487	0.248	1.056	3.907	7.814	5.139	10.286
40	1.257	2.513	0.329	1.129	3.086	6.171	2.309	4.621
42	0.073	5.106	1.088	2.976	4.693	6.628	5.254	5.279

TABLE 4

FREQUENCY SPECTRUM OF OUTPUT VOLTAGE
AMPLITUDE EXPRESSED AS A PERCENTAGE OF CORRESPONDING AVERAGE VALUE

UNBALANCED SUPPLY, $V_{ab} = 1.662/\underline{-27.33°}$, $V_{bc} = 1.527/\underline{88.29°}$,
$V_{ca} = 1.703/\underline{-153.38°}$

Harmonic Order n	SCHEME 1		SCHEME 2		SCHEME 3		SCHEME 4	
	V_N=1	V_N=.5	V_N=1	V_N=.5	V_N=1	V_N=.5	V_N=1	V_N=.5
2	9.801	19.602	9.801	9.8	9.806	19.612	9.806	19.611
4	1.797	3.594	0.021	0.057	0.014	0.028	0	0
6	5.494	57.368	0.39	1.31	0.527	0.679	0	0.014
8	4.403	8.806	0.064	0.214	0.125	0.249	0	0
10	2.144	4.287	0.049	0.214	0.326	0.652	0	0
12	1.194	24.788	0.397	1.638	3.245	3.606	8.994	18.001
14	3.986	7.972	0.128	0.541	1.262	2.524	5.468	10.937
16	1.919	3.838	0.12	0.555	0.097	0.194	9.556	19.112
18	0.424	13.209	0.737	2.863	4.542	8.488	2.824	64.608
20	3.703	7.407	0.503	1.738	4.466	8.932	17.709	35.419
22	1.547	3.094	4.042	2.336	0.894	1.789	1.179	2.359
24	0.167	6.97	6.964	31.838	6.345	9.293	1.429	3.358
26	3.369	6.739	21.766	50.199	8.98	17.961	0.284	0.569
28	1.149	2.298	8.61	19.872	8.897	17.795	4.157	8.314
30	0.064	3.389	4.248	19.416	1.456	24.591	0.555	13.615
32	2.972	5.943	10.418	6.211	20.007	40.014	13.234	26.468
34	0.815	1.63	0.241	0.826	2.441	4.882	0.826	1.652
36	0.038	2.285	0.326	1.225	0.021	6.976	1.957	6.079
38	2.503	5.006	0.496	2.108	7.857	15.714	10.34	20.68
40	0.667	1.335	0.17	0.598	1.629	3.259	1.221	2.443
42	0.038	2.927	0.624	1.709	2.691	3.8	3.012	3.025

4.7 Lower Order Harmonics

The lower order harmonic component in input line current requires larger size filter. Although a distortion factor gives an overall idea of harmonic components in input current, the specific knowledge about order and relative amplitude of lower order harmonic components give a better idea about the input filtering requirement.

Fig. 4.16 through Fig. 4.19 show the relative amplitude of lower order harmonics in input current of the converter for balanced supply. Fig. 4.20 through Fig. 4.31 show the relative amplitude of lower order harmonics for unbalanced supply conditions. For balanced supply, triplen harmonic components are not generated at the input. But under unbalanced supply condition triplen harmonic conponents become part of the input current. The relative amplitude of third harmonic component generated by scheme 2 is less than other schemes under unbalanced supply condition.

4.8 Switching Loss

The turn-on and turn-off of any semiconductor switch are associated with some loss. The implementation of force commutation with thyristors requires an extra commutation circuitry. Thus all the schemes are susceptible to commutation and switching losses. With the increase of pulse number per half cycle, these losses increase proportionally.

Recently developed gate-turn-off (GTO) thyrsitors do not require any external commutation circuitry. This makes the implementation of force-commutated converter structure easier. Table 5 shows the switching loss of different schemes using GTO thyristor as a switch. In calculating switching losses following data are assumed [20] to be the same for all

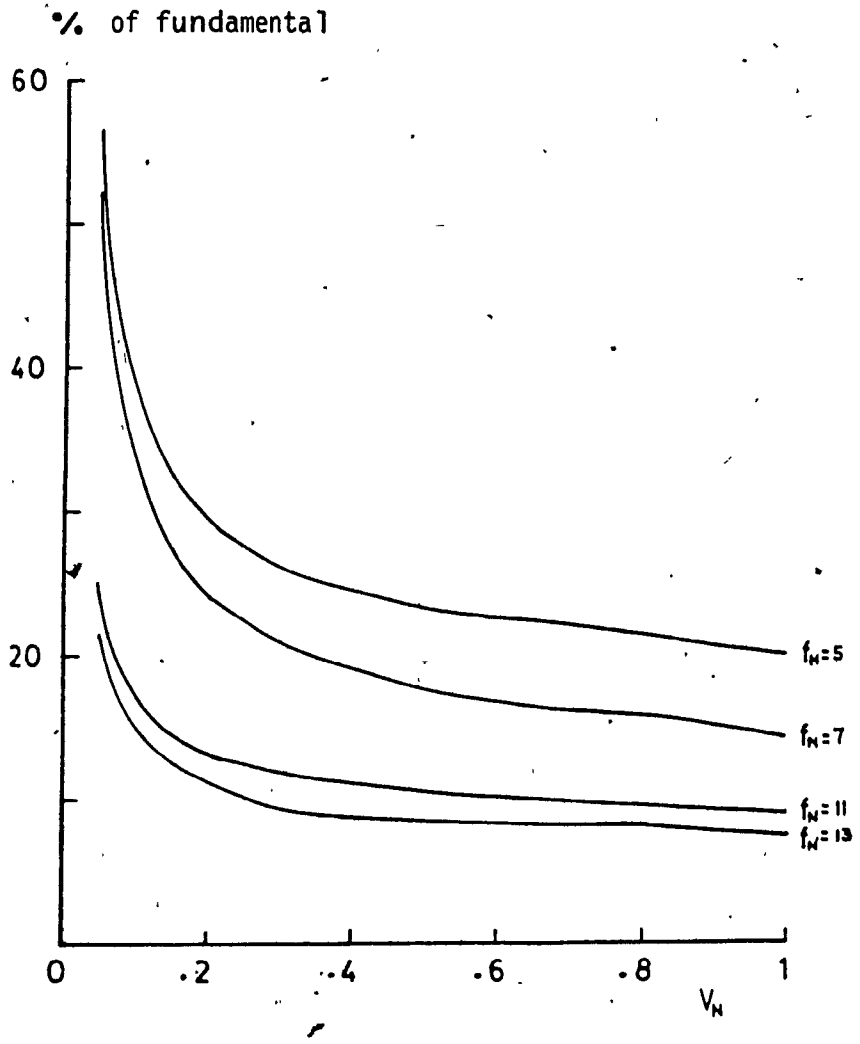

Fig. 4.16 Lower order harmonic component (input current) of Angle-controlled switching scheme. (Balanced supply)

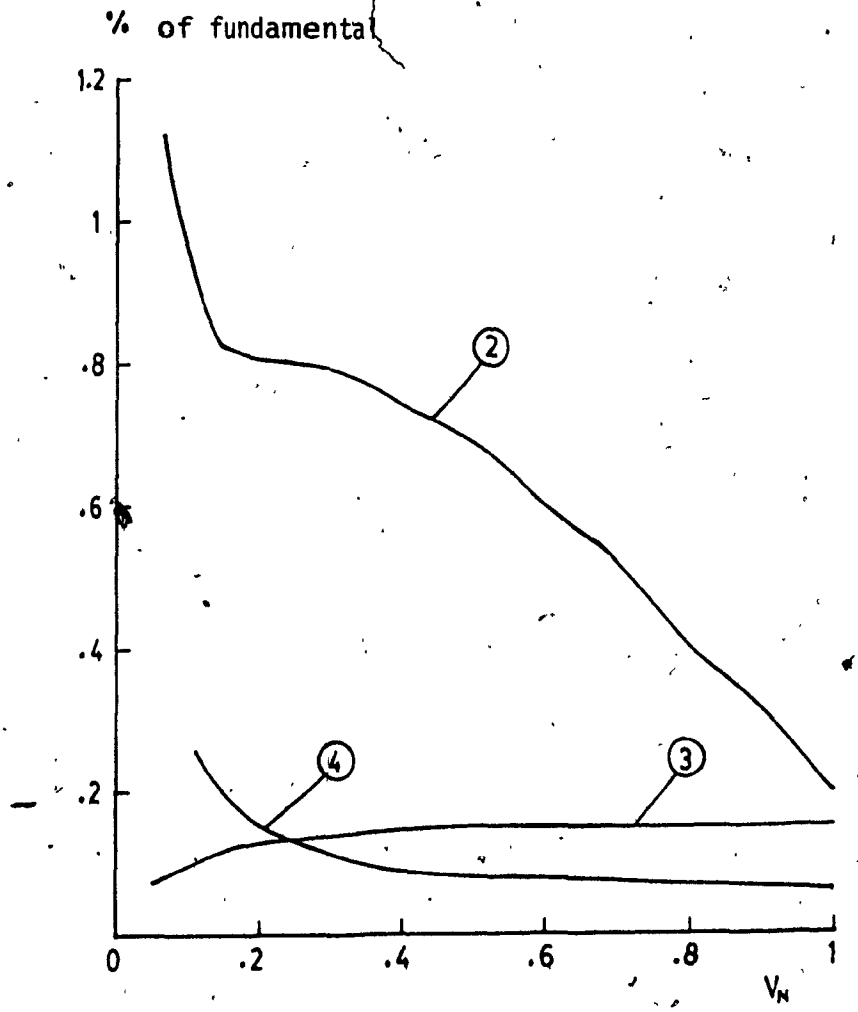

Fig. 4.17 5th harmonic component (input current) of different schemes. (Balanced supply)

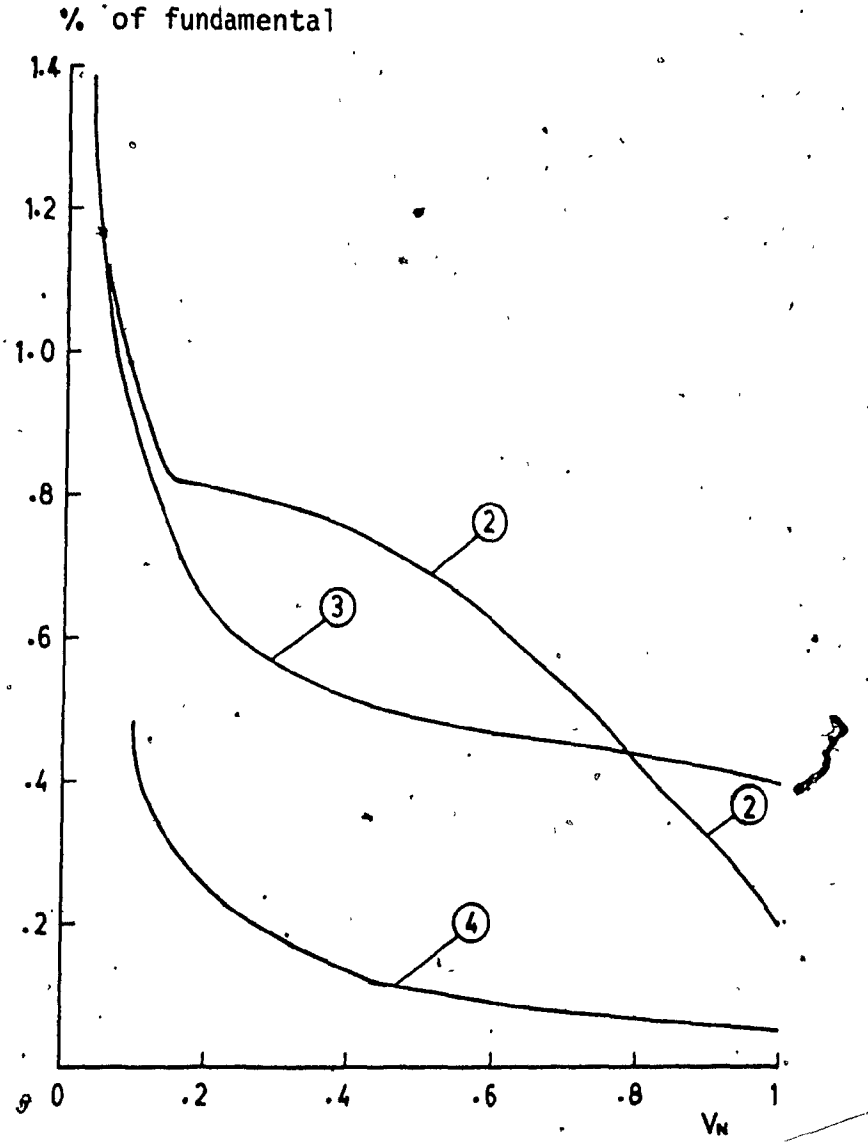

Fig. 4.18 7th harmonic component (input current) of different schemes. (Balanced supply)

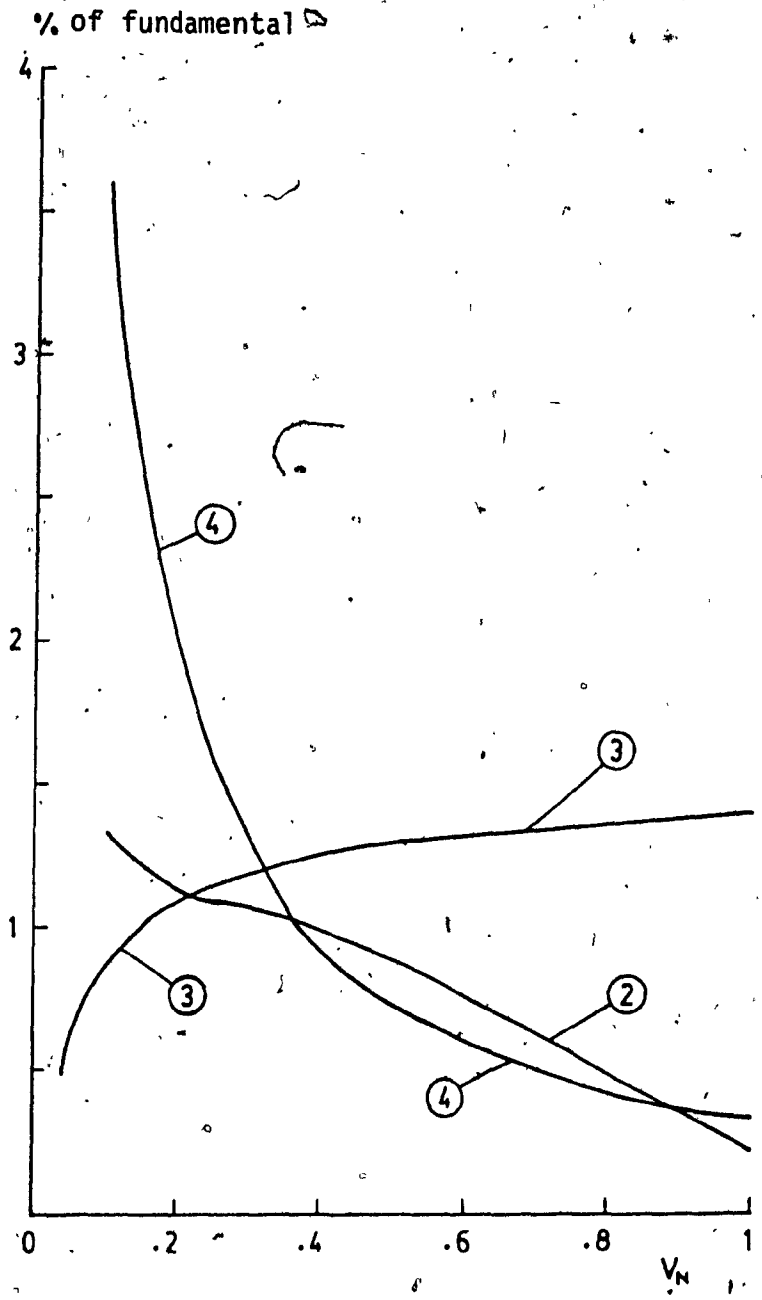

Fig. 4.19 11th harmonic component (input current) of different schemes. (Balanced supply)

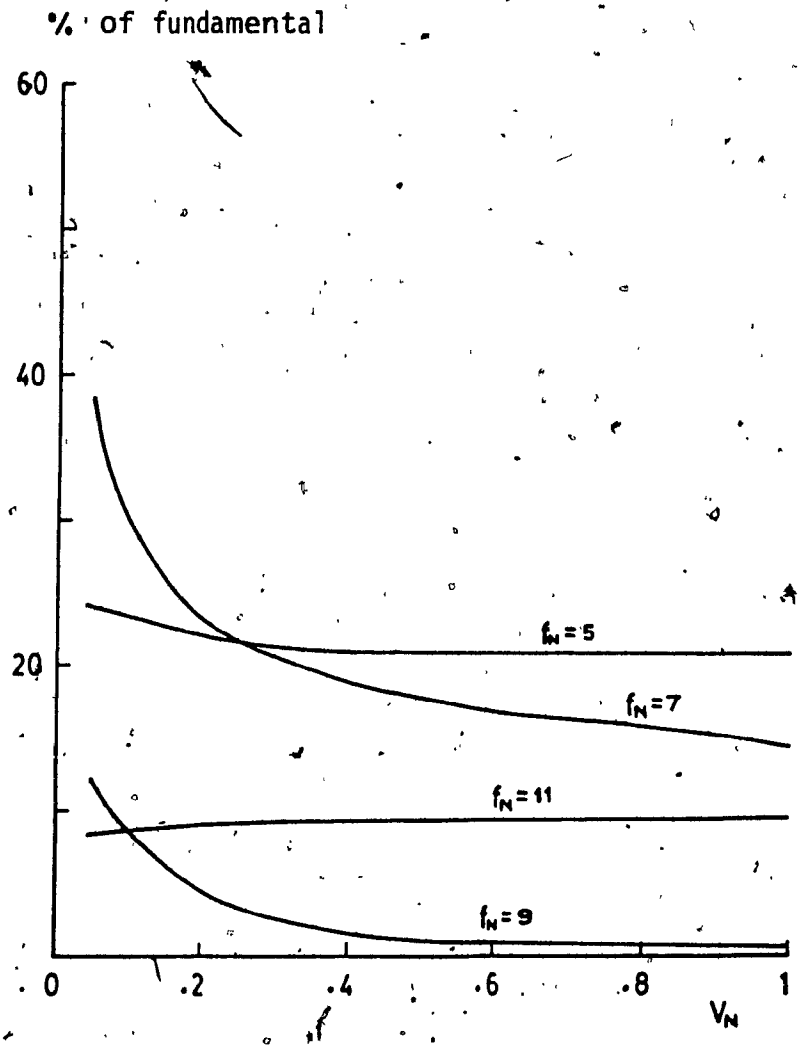

Fig. 4.20 Lower order harmonic component (input current) of angle-controlled switching scheme. (Unbalanced supply. $V_{ab} = 1.546\underline{/-27.18°}$, $V_{bc} = 1.432\underline{/80.06°}$, $V_{ca} = 1.769\underline{/-156.54°}$)

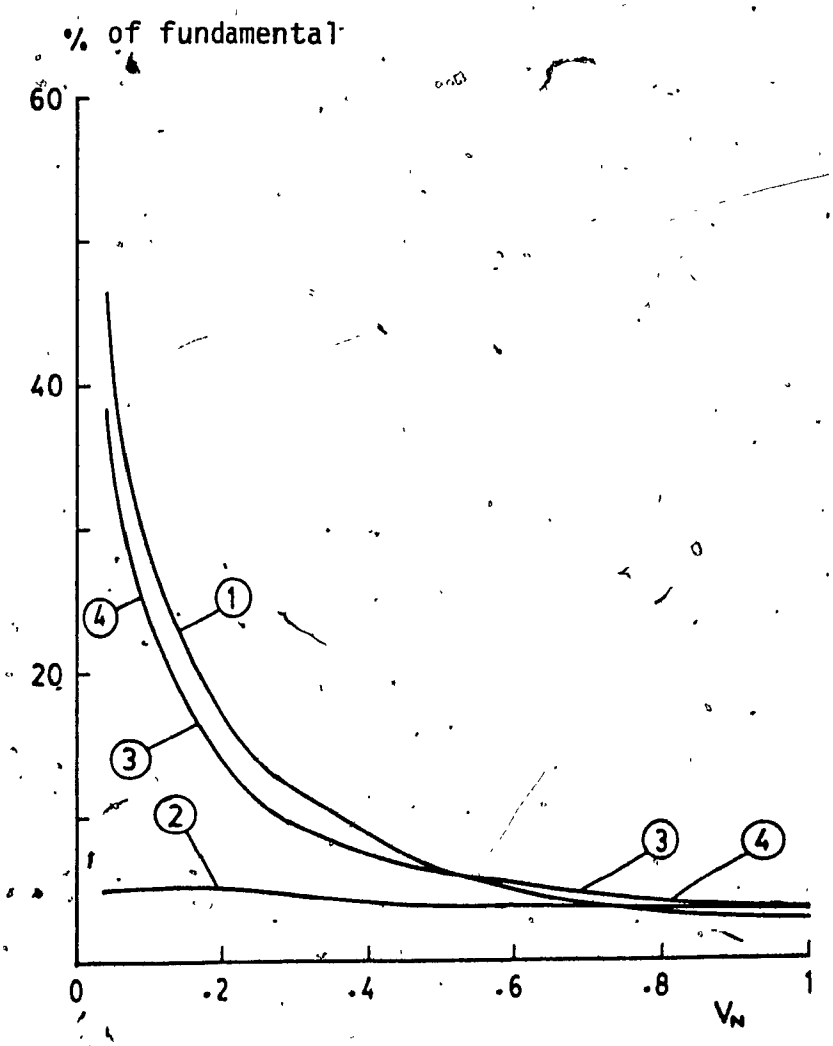

Fig. 4.21 3rd harmonic component (input current) of different schemes. (Unbalanced supply. $V_{ab} = 1.546/-27.18°$, $V_{bc} = 1.432/80.06°$, $V_{ca} = 1.769/-156.54°$)

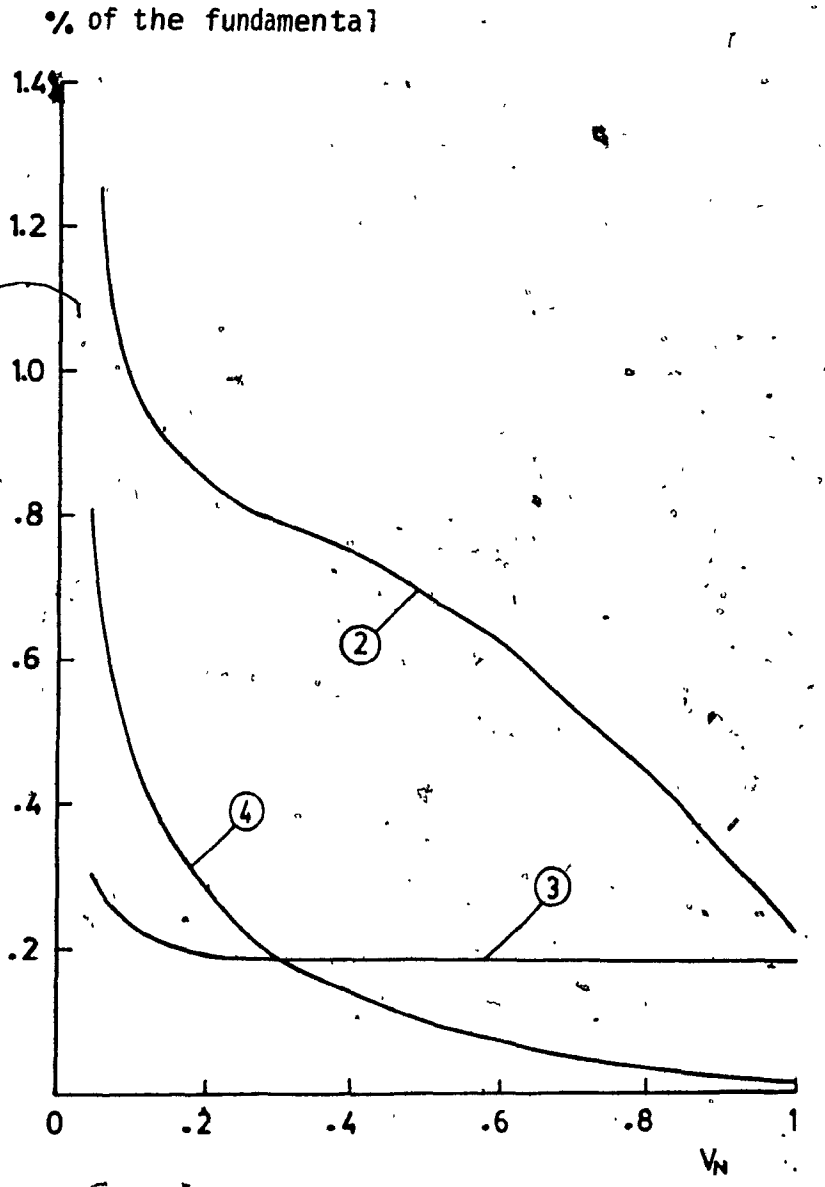

Fig. 4.22 5th harmonic component (input current) of different schemes. (Unbalanced supply. $V_{ab} = 1.546/\underline{-27.18°}$, $V_{bc} = 1.432/\underline{80.06°}$, $V_{ca} = 1.769/\underline{-156.54°}$)

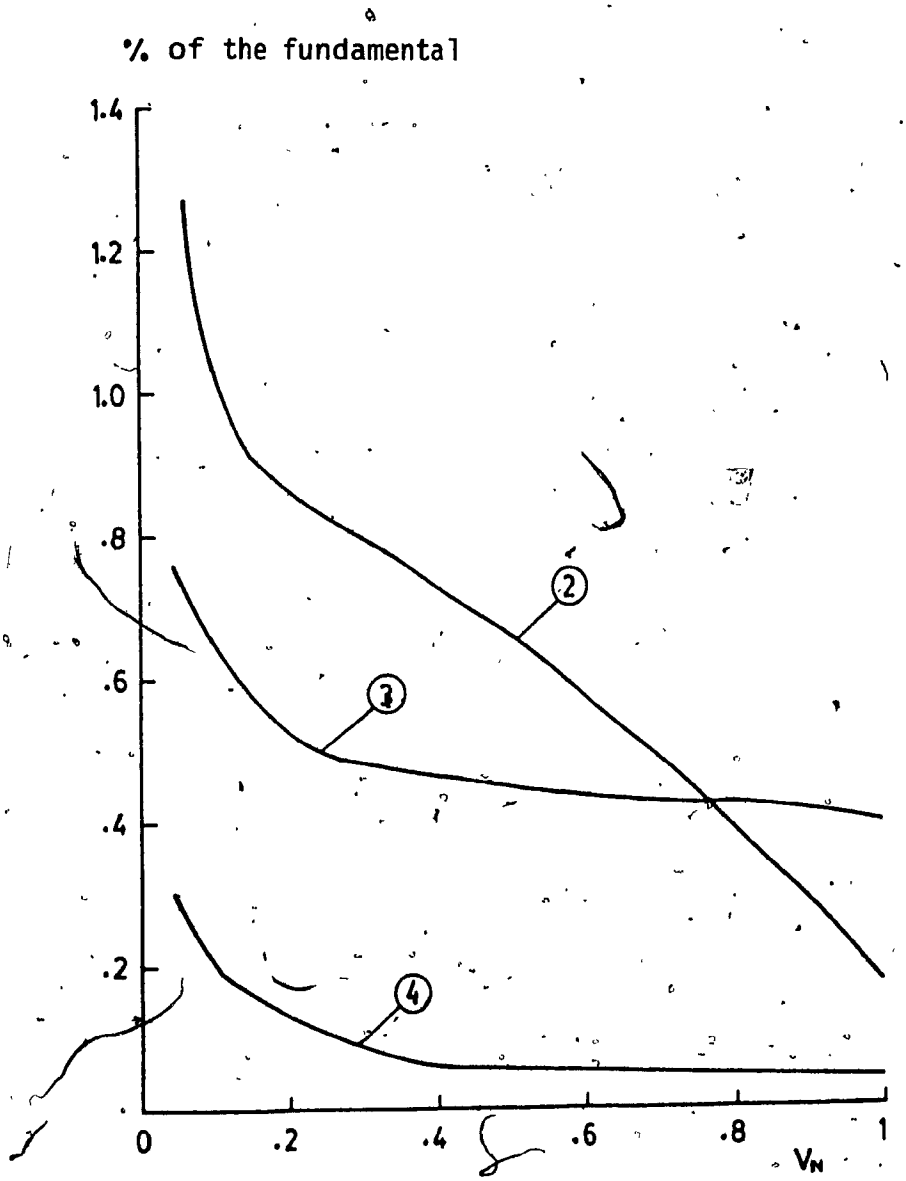

Fig. 4.23 7th harmonic component (input current) of different schemes. (Unbalanced supply. $V_{ab} = 1.546\underline{/-27.18°}$, $V_{bc} = 1.432\underline{/80,06°}$, $V_{ca} = 1.769\underline{/-156.54°}$)

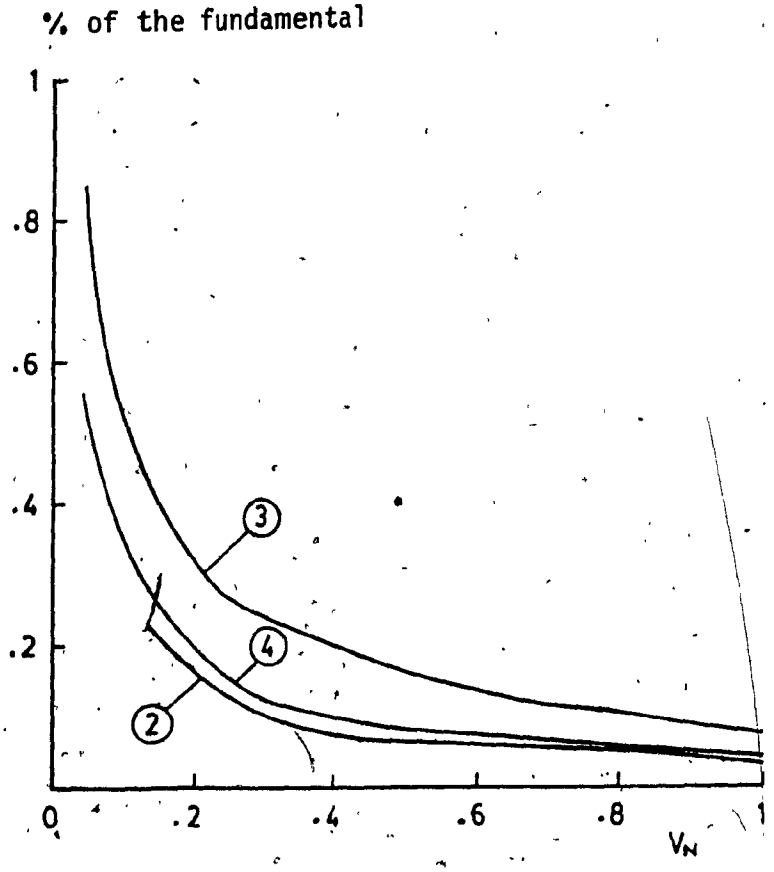

Fig. 4.24 9th harmonic component (input current) of different schemes. (Unbalanced supply. $V_{ab} = 1.546\underline{/-27.18°}$, $V_{bc} = 1.432\underline{/80.06°}$, $V_{ca} = 1.769\underline{/156.54°}$)

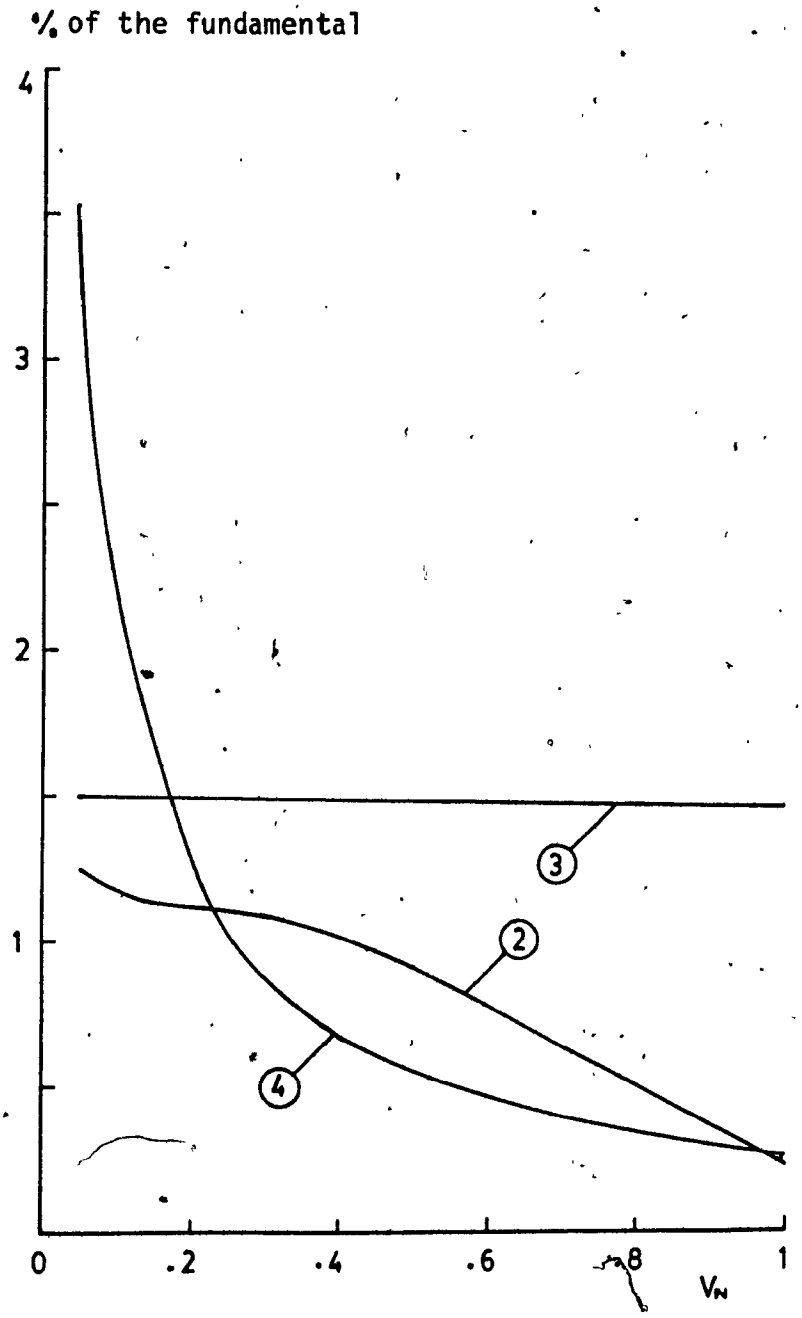

Fig. 4.25 11th harmonic component (input current) of different schemes. (Unbalanced supply. $V_{ab} = 1.546/\underline{-27.18°}$, $V_{bc} = 1.432/\underline{80.06°}$, $V_{ca} = 1.769/\underline{-156.54°}$)

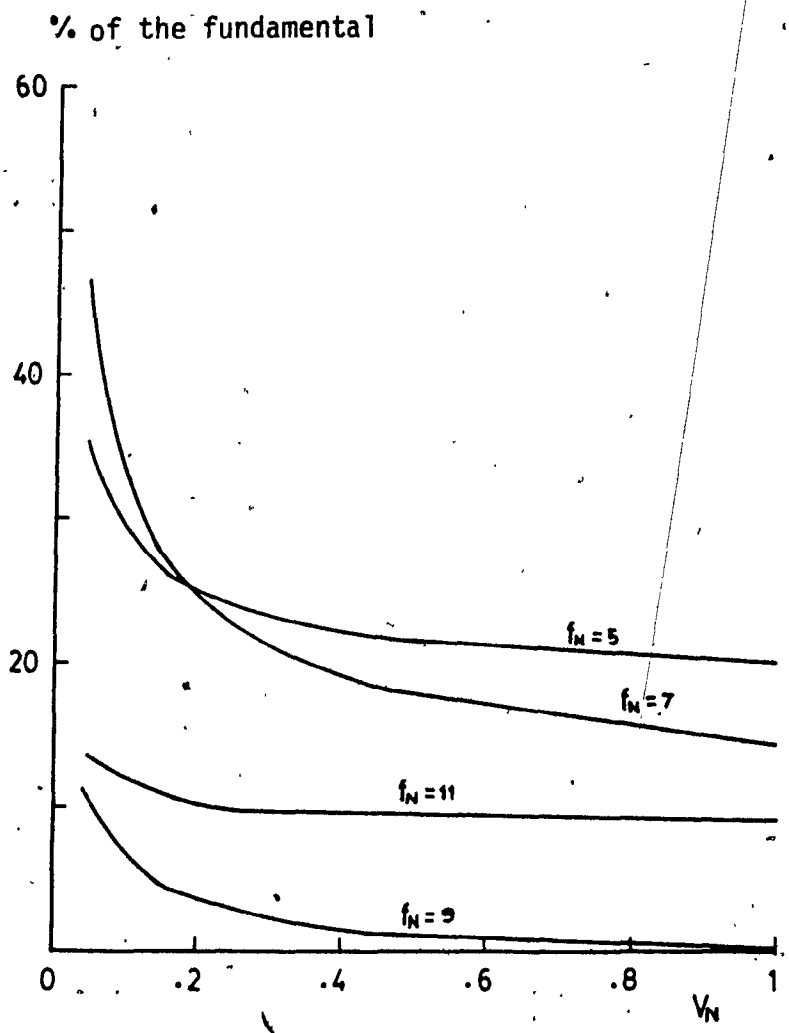

Fig. 4.26 Lower order harmonic component (input current) of angle-controlled switching scheme. (Unbalanced supply. $V_{ab} = 1.662/\underline{-27.33°}$, $V_{bc} = 1.527/\underline{88.29°}$, $V_{ca} = 1.703/\underline{-153.38°}$)

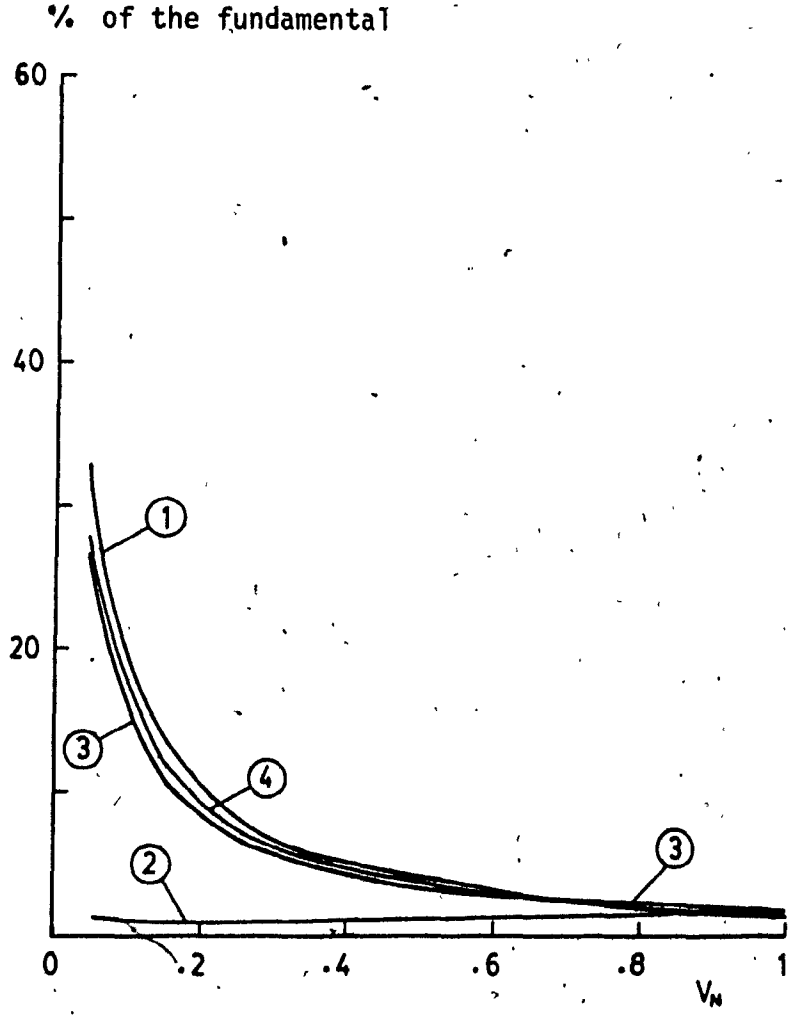

Fig. 4.27 3rd harmonic component (input current) of different schemes. (Unbalanced supply. $V_{ab} = 1.662/\underline{-27.33°}$, $V_{bc} = 1.527/\underline{88.29°}$, $V_{ca} = 1.703/\underline{-153.38°}$)

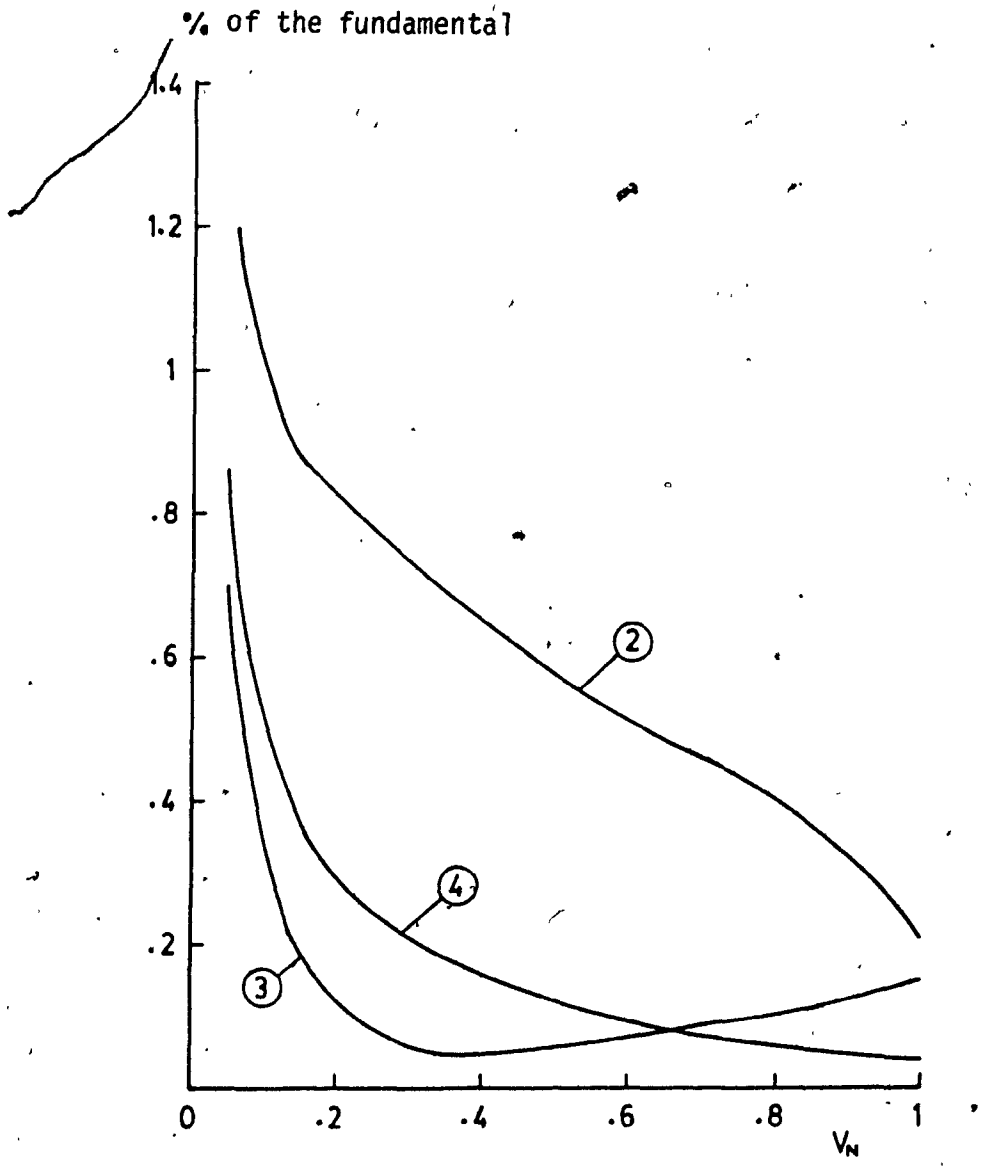

Fig. 4.28 5th harmonic component (input current) of different schemes. (Unbalanced supply. $V_{ab} = 1.662/\underline{-27.33°}$, $V_{bc} = 1.527/\underline{88.29°}$, $V_{ca} = 1.703/\underline{-153.38°}$)

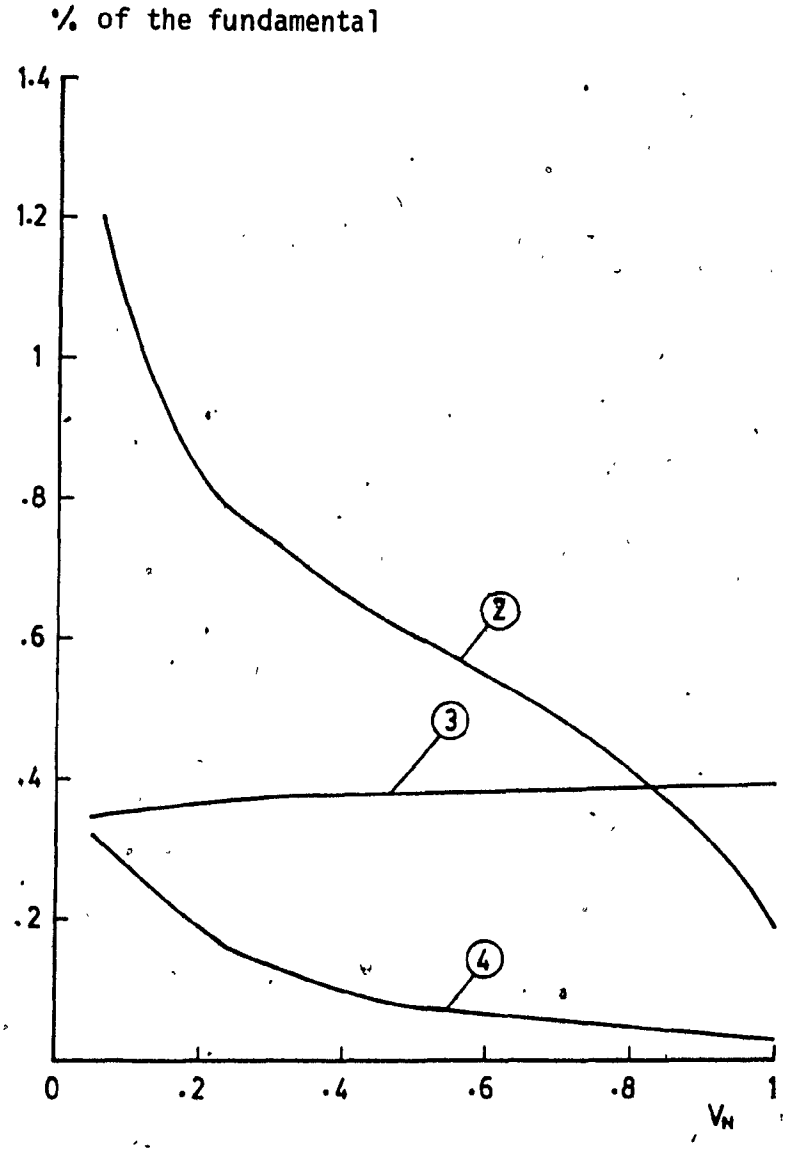

Fig. 4.29 7th harmonic component (input current) of different schemes. (Unbalanced supply. $V_{ab} = 1.662\underline{/-27.33°}$, $V_{bc} = 1.527\underline{/88.29°}$, $V_{ca} = 1.703\underline{/-153.38°}$)

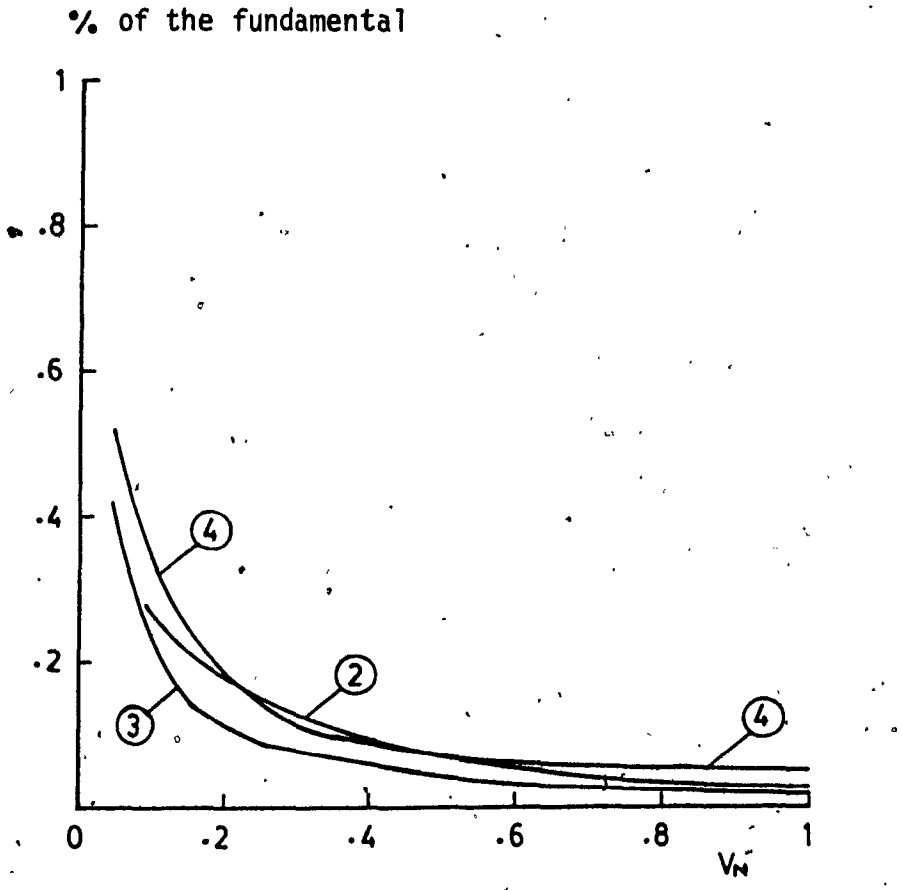

Fig. 4.30 9th harmonic component (input current) of different schemes. (Unbalanced supply. $V_{ab} = 1.662\underline{/-27.33°}$, $V_{bc} = 1.527\underline{/88.29°}$, $V_{ca} = 1.703\underline{/-153.38°}$)

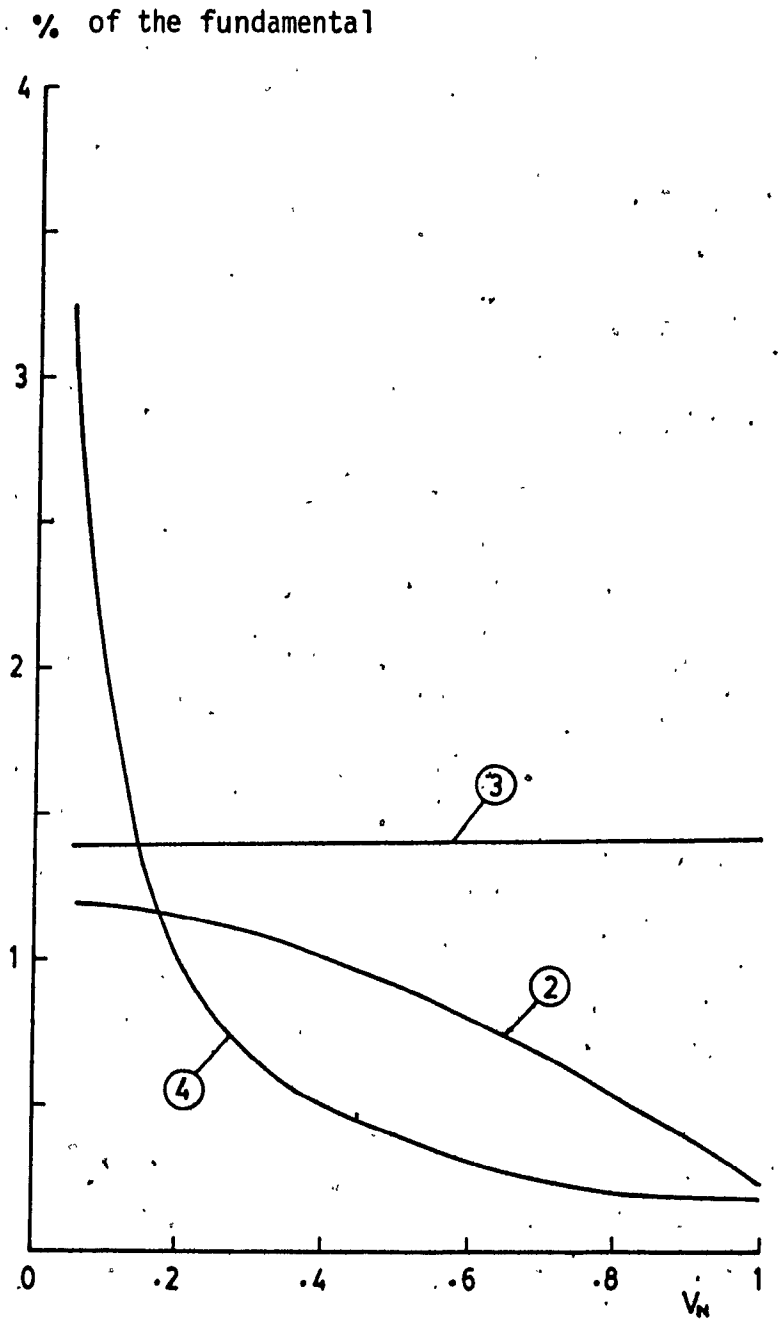

Fig. 4.31 11th harmonic component (input current) of different schemes. (Unbalanced supply. $V_{ab} = 1.662/\underline{-27.33°}$, $V_{bc} = 1.527/\underline{88.29°}$, $V_{ca} = 1.703/\underline{-153.38°}$)

schemes.

Repetitive peak off-state voltage = 800 V

Repetitive controllable on-state current = 30A

On-pulse gate current = 4A

Rate of rise of on pulse gate current = 4 A/μs

Off-pulse reverse blocking gate voltage = 12V

Snubber capacitor = .022 μF

TABLE 5

Scheme	N_p	Losses per pulse in Watt-sec	Switching loss in Watts
1	1	1.74	10.44
2	16	1.74	187.92
3	11	1.74	114.84
4	7	1.74	73.08

CHAPTER 5

CONCLUSIONS

From the frequency spectrum of output voltage in Table 2 (Section 4.6), it is evident that the PWM switching schemes 2,3 and 4 designed to improve the waveshape of input line current, should require smaller output filter in comparison to line commutated converter (scheme 1) under normal (balanced) supply condition. In practice, the converter loads are inductive, and this inductance would help the output current become smoother. From Table 3 and 4 (Section 4.6) it is clear that under unbalanced supply conditions second harmonic component will appear in significant proportion at the output of all four schemes. Thus an output filter designed for normal supply, will not be able to suppress the second harmonic component resulted from unbalanced supply.

The input power factor of the modified sinusoidal PWM scheme (scheme 2) was found better than other schemes over most of the operating range. This improved feature exists for both balanced and unbalanced supply conditions (Figs. 4.6, 4.7 and 4.8). Although the angle controlled scheme showed improved power factor over other schemes near rated voltage, the obvious choice is modified sinusoidal PWM scheme from power factor point of view. The power factors of other three schemes are not significantly different from each other. Although specific harmonic elimination scheme (scheme 4) showed least distortion of the input current over other scheme under balanced supply, it is the modified sinusoidal PWM scheme which showed least input current distortion under unbalanced supply condition.

Under unbalanced supply conditions, triplen harmonic component appears at the input. It is evident from Section 4.7 that 3rd order harmonic component appears at the input line current in significant proportion in all schemes except modified sinusoidal PWM scheme whenever the supply becomes unbalanced. In modified sinusoidal PWM scheme this 3rd harmonic component is not significant. An input filter originally designed by considering supply feature as balanced, will not be able to suppress this 3rd harmonic component successfully. Therefore, it is better to use modified sinusoidal PWM scheme where there is a possibility of the supply to be unbalanced.

The reduction or elimination of lower order harmonics would shift the dominant harmonics to higher order and the filter size would be reduced. Any further shift towards higher order may not be desirable, because at this point the radiated EMI problem might be significant.

With the introduction of Gate Turn-off thyristors, the implementation of force commutation does not require an extra commutation circuitry. Thus converter with PWM scheme can be built with less weight using GTO thyristors. However, any PWM scheme has its increased switching loss in comparison to conventional angle controlled scheme. But this switching loss should be weighted against the gains earned.

This study shows the comparative analysis of four different switching schemes. It gives a guideline to select a particular switching scheme depending on operating criteria. This study also shows the effect of unbalanced supply on converter operation. Unbalanced supply produces undesirable lower order harmonic components both at the input and output of the converter. There is no known switching scheme which can operate

under unbalanced supply without producing these lower order harmonic components.

Future study:

1) This study can be extended to develop a future switching scheme which would minimize and/or maximize certain criterion under balanced and unbalanced supply conditions.

2) This study can also be used as a basis for finding an adaptive switching scheme which would handle supply unbalances keeping performance degradation within some tolerance. However, the quantitative limit of this tolerance is yet to be decided by additional future work.

3) This study is based on the assumption of ideal switching scheme. In practice, there is a delay in switching 'on' and 'off' of the power semiconductor switches. This delay will change the results of this study. The results of the imperfections of the switches may also be investigated.

4) This work can be extended to study the effects of power factor degradation and converter-generated harmonics on the transformers in a power systems under balanced and unbalanced supply conditions.

APPENDIX A

DETERMINATION OF INPUT AND OUTPUT CURRENT AND OUTPUT VOLTAGE BY EXACT ANALYSIS

A.1 Output Voltage

The transfer function of a converter $S(\theta)$ can be expressed in terms of it's Fourier series components as

$$S(\theta) = \sum_{n=1}^{\infty} H_n \sin(n\theta + \psi_n) \qquad (A.1)$$

Assuming $S_1(\theta)$, $S_2(\theta)$, $S_3(\theta)$, ... $S_6(\theta)$ as the corresponding gating functions as applied to each switches, the transfer functions with respect to the input ports of the converter becomes $[S_1(\theta) - S_6(\theta)]$, $[S_3(\theta) - S_2(\theta)]$ and $[S_5(\theta) - S_4(\theta)]$.

Assuming the supply phase voltage as

$$v_1 = E_1 \sin(\theta - \phi_1)$$

$$v_2 = E_2 \sin(\theta - \phi_2)$$

$$v_3 = E_3 \sin(\theta - \phi_3)$$

output voltage expression becomes

$$v_0(\theta) = \{v_i(\theta)\}\{S(\theta)\} \qquad (A.2)$$

$$= \{S_1(\theta) - S_6(\theta)\}\, E_1 \sin(\theta - \phi_1)$$

$$+ \{S_3(\theta) - S_2(\theta)\}\, E_2 \sin(\theta - \phi_2)$$

$$+ \{S_5(\theta) - S_4(\theta)\} E_3 \sin(\theta - \phi_3)$$

or, $$v_0(\theta) = F_1(\theta) + F_2(\theta) + F_3(\theta) \qquad (A.3)$$

where:

$$F_1(\theta) = \{S_1(\theta) - S_6(\theta)\} E_1 \sin(\theta - \phi_1)$$

$$F_2(\theta) = \{S_3(\theta) - S_2(\theta)\} E_2 \sin(\theta - \phi_2)$$

$$F_3(\theta) = \{S_5(\theta) - S_4(\theta)\} E_3 \sin(\theta - \phi_3)$$

Using respective Fourier series for the transfer functions $F_1(\theta)$, $F_2(\theta)$ and $F_3(\theta)$ can be expressed as

$$F_1(\theta) = E_1 \sin(\theta - \phi_1) \sum_{n=1}^{\infty} H_n \sin(n\theta - n\alpha - n\phi_1) \qquad (A.4)$$

$$F_2(\theta) = E_2 \sin(\theta - \phi_2) \sum_{n=1}^{\infty} H_n \sin(n\theta - n\alpha - n\phi_2) \qquad (A.5)$$

$$F_3(\theta) = E_3 \sin(\theta - \phi_3) \sum_{n=1}^{\infty} H_n \sin(n\theta - n\alpha - n\phi_3) \qquad (A.6)$$

where α = phase displacement angle

The output voltage components can be rewritten by using simple trigonometrical identity.

$$F_1(\theta) = \sum_{n=1}^{\infty} \frac{E_1 H_n}{2} [\cos\{(n-1)\theta - (n-1)\phi_1 - n\alpha\}$$

$$- \cos\{(n+1)\theta - (n+1)\phi_1 - n\alpha\}] \qquad (A.7)$$

$$F_2(\theta) = \sum_{n=1}^{\infty} \frac{E_2 H_n}{2} [\cos\{(n-1)\theta - (n-1)\phi_2 - n\alpha\} - \cos\{(n+1)\theta - (n+1)\phi_2 - n\alpha\}] \quad (A.8)$$

$$F_3(\theta) = \sum_{n=1}^{\infty} \frac{E_3 H_n}{2} [\cos\{(n-1)\theta - (n-1)\phi_3 - n\alpha\} - \cos\{(n+1)\theta - (n+1)\phi_3 - n\alpha\}] \quad (A.9)$$

Using Eqns. A.7, A.8 and A.9 for $n=1$, output dc voltage becomes

$$V_{dc} = \tfrac{1}{2}(E_1 + E_2 + E_3) H_1 \cos \alpha \quad (A.10)$$

Substituting $n=1,2,3,4,\ldots$ in the Eqns. A.7, A.8 and A.9 the corresponding output voltage harmonic components are:

First harmonic component, $v_{01} = 0$

2nd harmonic component,

$$v_{02} = \frac{E_1 H_3}{2} \cos(2\theta - 2\phi_1 - 3\alpha) - \frac{E_1 H_1}{2} \cos(2\theta - 2\phi_1 - \alpha) + \frac{E_2 H_3}{2} \cos(2\theta - 2\phi_2 - 3\alpha) - \frac{E_2 H_1}{2} \cos(2\theta - 2\phi_2 - \alpha) + \frac{E_3 H_3}{2} \cos(2\theta - 2\phi_3 - 3\alpha) - \frac{E_3 H_1}{2} \cos(2\theta - 2\phi_3 - \alpha)$$

3rd harmonic component,

$$v_{03} = \frac{E_1 H_4}{2} \cos(3\theta - 3\phi_1 - 4\alpha) - \frac{E_1 H_2}{2} \cos(3\theta - 3\phi_1 - 2\alpha) + \frac{E_2 H_4}{2} \cos(3\theta - 3\phi_2 - 4\alpha) - \frac{E_2 H_2}{2} \cos(3\theta - 3\phi_2 - 2\alpha) + \frac{E_3 H_4}{2} \cos(3\theta - 3\phi_3 - 4\alpha) - \frac{E_3 H_2}{2} \cos(3\theta - 3\phi_3 - 2\alpha)$$

Similarly mth harmonic component of the output voltage can be written as

$$v_{o_m} = \frac{E_1 H_{m+1}}{2} \cos\{m\theta - m\phi_1 - (m+1)\alpha\} - \frac{E_1 H_{m-1}}{2} \cos\{m\theta - m\phi_1 - (m-1)\alpha\}$$
$$+ \frac{E_2 H_{m+1}}{2} \cos\{m\theta - m\phi_2 - (m+1)\alpha\} - \frac{E_2 H_{m-1}}{2} \cos\{m\theta - m\phi_2 - (m-1)\alpha\}$$
$$+ \frac{E_3 H_{m+1}}{2} \cos\{m\theta - m\phi_3 - (m+1)\alpha\} - \frac{E_3 H_{m-1}}{2} \cos\{m\theta - m\phi_3 - (m-1)\alpha\} \quad (A.11)$$

A.2 Output Current

Load impednace to the mth output voltage harmonic component is

$$Z_m \underline{/\sigma_m} = \{R^2 + (2m\pi f L)^2\}^{\frac{1}{2}} \underline{/\tan^{-1}}\left(\frac{2m\pi fL}{R}\right)$$

Output average current, $I_{dc} = \frac{V_{dc}}{R} - \frac{E_c}{R}$

Considering a specific voltage harmonic component and it's corresponding impedance term, the harmonic components of output current can be evaluated. After combining all the harmonic components, the output current of the converter can be expressed as

$$i_o(\theta) = I_{dc} + \sum_{n=1}^{\infty} I_n \sin(n\theta + \beta_n) \quad (A.12)$$

A.3 Input Line Current

Assuming no losses in the converter, instantaneous input power is equal to the instantaneous output power.

$$\{v_i(\theta)\}\{i_i(\theta)\} = \{v_o(\theta)\}\{i_o(\theta)\} \quad (A.13)$$

From Eqn. A.2, $v_o(\theta)$ can be expressed in terms of input voltage.

i.e., $\{v_i(\theta)\}\{i_i(\theta)\} = \{v_i(\theta)\}\{S(\theta)\}\{i_o(\theta)\}$

or, $$i_i(\theta) = \{S(\theta)\}\{i_o(\theta)\} \qquad (A.14)$$

Therefore, instantaneous input line current,

$$i_i(\theta) = \{\sum_{m=1}^{\infty} H_m \sin(m\theta + \psi_m)\}\{I_{dc} + \sum_{n=1}^{\infty} I_n \sin(n\theta + \beta_n)\}$$

$$= I_{dc} \sum_{m=1}^{\infty} H_m \sin(m\theta + \psi_m) + \{\sum_{m=1}^{\infty} \sum_{n=1}^{\infty} \frac{H_m I_n}{2} [\cos\{(n-m)\theta + \beta_n - \psi_m\}$$

$$- \cos\{(n+m)\theta + \beta_n + \psi_m\}] \qquad (A.15)$$

It is clear from Eqn. A.15 that it's first term contributes a kth harmonic component for $m=K$. The second term contributes kth harmonic component for the following cases

when:

$$\left.\begin{array}{lll} n - m = K & \text{i.e.,} & n = K + m \\ n + m = K & \text{i.e.,} & n = K - m \\ n - m = -K & \text{i.e.,} & m = n + K \end{array}\right\} \qquad (A.16)$$

An expression for kth harmonic component of input line current can be obtained by substituting Eqns. A.16 in Eqn. A.15.

$$i_{i,k}(\theta) = I_{dc} H_k \sin(K\theta + \psi_k)$$

$$+ \sum_{m=1}^{\infty} \frac{H_m I_{k+m}}{2} \cos(K\theta + \beta_{k+m} - \psi_m)$$

$$- \sum_{m=1}^{k-1} \frac{H_m I_{k-m}}{2} \cos(K\theta + \beta_{k-m} + \psi_m)$$

$$+ \sum_{n=1}^{\infty} \frac{H_{n+k} I_n}{2} \cos(-K\theta + \beta_n - \psi_{n+k}) \qquad \text{(A.17)}$$

Third term in expression (A.17) contributes from second harmonic component to higher order harmonic components.

APPENDIX B

DERIVATION OF SWITCHING FUNCTION FOR OPTIMUM DISTORTION FACTOR

The switching function for optimum input current distortion factor is derived by considering the output current of the converter to be ripple free. Thus the input line current becomes identical to the switching function. The distortion factor (DF) can be expressed as,

$$DF = \frac{\left[\sum_{n=2}^{\infty} (H_n/n^2)^2\right]^{\frac{1}{2}}}{H_1} \times 100 \qquad (B.1)$$

The switching function for the optimum distortion factor can have different number of pulses per half cycle. Each switching function has its own minimum DF depending on the pulse number. In general DF decreases with the increase of pulse number. Once the number of pulses per half cycle is chosen, assuming an odd switching function with quarter wave symmetry; H_n of the switching function becomes,

$$H_n = \frac{4}{\pi} \int_0^{\pi/2} S(\theta)\ n\theta\ d\theta \qquad (B.2)$$

or, $$H_n = \frac{4}{n\pi} [\cos(nT_1) - \cos(nT_2) + \cos(nT_3) - \cos(nT_4) \ldots\ldots$$

$$\ldots + \cos(nT_m)] \qquad (B.3)$$

[Note: $S(\theta)$ can be either '0' or '1' depending on switching interval].

where,

T_m = mth switching angle, rad and $m = N_p$

From Eqn. B.3 it is clear that all harmonic components of the switching function become the function of switching angles. For example, the harmonic components of a switching function with 5 pulses per half cycle are

$$H_1 = \frac{4}{\pi} [\cos T_1 - \cos T_2 + \cos T_3 - \cos T_4 + \cos T_5]$$

$$H_3 = \frac{4}{3\pi} [\cos 3T_1 - \cos 3T_2 + \cos 3T_3 - \cos 3T_4 + \cos 3T_5]$$

$$H_5 = \frac{4}{5\pi} [\cos 5T_1 - \cos 5T_2 + \cos 5T_3 - \cos 5T_4 + \cos 5T_5]$$

and so on.

Once the harmonic components of the switching function are known Eqn. B.1 can be used to determine the corresponding DF.

A computer program named 'OPT' was deveoped to calculate the DF for all possible combinations of switching angles. From these calculated values of DF, the switching angles for minimum DF were selected. These switching angles then formed the required switching function for optimum distortion factor.

APPENDIX C

DERIVATION OF SWITCHING FUNCTION FOR SPECIFIC HARMONIC ELIMINATION

The switching function which eliminates specific harmonic components from the input current of a converter is derived by considering the output current of the converter to be ripple free. Thus the input line current becomes identical to the switching function. The switching function for specific harmonics elimination can have different number of pulses per half cycle. The switching function is assumed to be odd with quarter wave symmetry. Considering the constraints of output current continuity, the switching function can eliminate $(N_p-1)/2$ number of harmonic components. Thus a system of equations can be generated in the following way.

$$H_n = \frac{4}{\pi} \int_0^{\pi/2} S(\theta) \sin n\theta \, d\theta = 0 \qquad (C.1)$$

[Note: $S(\theta)$ can be either '0' or '1' depending on switching interval]

where n is the order of the harmonic component which is to be eliminated. Depending on the number of pulses per half cycle 'n' can have different values.

For example, if we have a switching function of 5 pulses per half cycle, we can eliminate 2 harmonic components, 5th and 7th (say). The corresponding two equations will be of the following form.

$$H_5 = \frac{4}{\pi} \int_0^{\pi/2} S(\theta) \sin 5\theta \, d\theta = 0 \qquad (C.2)$$

$$H_7 = \frac{4}{\pi} \int_0^{\pi/2} S(\theta) \sin 7\theta \, d\theta = 0 \qquad (C.3)$$

Eqns. C.2 and C.3 can be rewritten as

$$H_5 = \frac{4}{5\pi} [\cos(5T_1) - \cos(5T_2) + \cos(5T_3) - \cos(5T_4) + \cos(5T_5)] = 0 \qquad (C.4)$$

and

$$H_7 = \frac{4}{7\pi} [\cos(7T_1) - \cos(7T_2) + \cos(7T_3) - \cos(7T_4) + \cos(7T_5)] = 0 \qquad (C.5)$$

For the constraints of output current continuity, $T_3 = 30°$ and T_4 and T_5 are dependent variables. The solution of Eqns. C.4 and C.5 will give the required switching angles of the switching function to eliminate 5th and 7th harmonic component of the input current.

A computer program named 'ELM' was developed to calculate the switching angles for specific harmonics elimination. Newton's method for nonlinear systems was used to solve the system of Eqns. C.1.

APPENDIX D

COMPUTATION OF DIFFERENT PERFORMANCE DATA

D.1 Unbalanced Supply

The distortion factor, input power factor, THD of output voltage and harmonic contents of input current and output voltage of converter for four switching schemes were computed for balanced and two unbalanced supply conditions. There is no established standard for the worst supply unbalance. The choice of two unbalanced supply for this study is arbitrary. Two cases of an unbalanced supply are considered in this study.

Case 1: $V_{an} = 1\underline{/0°}$ P.U., $V_{bn} = 0.8\underline{/118°}$ P.U. and $V_{cn} = 0.94\underline{/-131.5°}$ P.U.

Corresponding line voltages are:

$V_{ab} = 1.546\underline{/-27.18°}$ P.U., $V_{bc} = 1.432\underline{/80.06°}$ P.U.

and $V_{ca} = 1.769\underline{/-156.54°}$ P.U.

Case 2: $V_{an} = 1\underline{/0°}$ P.U., $V_{bn} = 0.9\underline{/122°}$ P.U.

and $V_{cn} = 0.93\underline{/-124.5°}$ P.U.

Corresponding line voltages are:

$V_{ab} = 1.662\underline{/-27.33°}$ P.U., $V_{bc} = 1.527\underline{/88.29°}$ P.U.

and $V_{ca} = 1.703\underline{/-153.38°}$ P.U.

Four computer programs for schemes 1,2,3 and 4 ('ACONT' for scheme 1, 'MSPWM' for scheme 2, 'ODF' for scheme 3 and 'SHELM' for scheme 4) were developed based on the analysis shown in Appendix A. These computer programs were used to compute the different performance data and frequency

spectrum of input current and output voltage of converter for both balanced and unbalanced supply conditions.

D.2 THD of Output Voltage

Eqn. A.11 in Appendix A gives the output voltage in terms of it's harmonic components. The computer programs as mentioned in previous section D.1 combined the like frequency terms of the output voltage. The THD was calculated by using the expression for THD given in Section 1.3.

D.3 Distortion Factor

Eqn. A.15 in Appendix A gives the input line current in terms of its harmonic components. The computer programs as mentioned in Section D.1 combined the like frequency terms of the input current. The DF was calculated by using the expression for DF given in Section 1.3.

D.4 Input Power Factor

Eqn. A.15 in Appendix A was used in the computer programs (ACONT, MSPWM, ODF and SHELM) to calculate the phase and RMS value of the fundamental component of the input current. The same equation was used to compute the amplitude of other harmonic components. The effective value of the input current was computed by using the fundamental and other harmonic components. Once the RMS value of the input current and phase and RMS value of it's fundamental component was known Eqn. 4.1 in Section 4.4 was used to compute the input power factor.

D.5 Frequency Spectrum

Eqns. A.11 and A.15 were used to compute the output voltage and input current in terms of it's Fourier coefficients. The computer programs (ACONT, MSPWM, ODF and SHELM) combined the like frequency terms.

REFERENCES

1. John R. Linders, "Electric Wave Distortions: Their Hidden Costs and Containment", IEEE Transactions on Industry Applications, Vol. IA-15, No. 5, September/October 1979, pp. 458-469.

2. Ray P. Stratford, "Rectifier Harmonics in Power Systems", IEEE Transactions on Industry Applications, Vol. IA-16, No. 2, March/April 1980, pp. 271-276.

3. David D. Shipp, "Harmonic Analysis and Suppression for Electrical Systems Supplying Static Power Converters and Other Nonlinear Loads", IEEE Transactions on Industry Applications, Vol. IA-15, No. 5, September/October 1979, pp. 453-458.

4. Ray P. Stratford, "Harmonic Pollution on Power Systems - A Change in Philosophy", IEEE Transactions on Industry Applications, Vol. IA-16, No. 5, September/October 1980, pp. 617-623.

5. James H. Galloway, "Harmonic Line Currents in Large Thyrsitor Six-Pulse Converters", IEEE Transactions on Industry Applications, Vol. IA-11, No. 3, May/June 1975, pp. 256-262.

6. Guy Olivier and V.R. Stefanovic, "Thyrsitor Current Source with an Improved Power Factor", IEEE Transactions on Industrial Electronics, Vol. IE-29, No. 4, November 1982, pp. 299-307.

7. D.E. Steeper and R.P. Stratford, "Reactive Compensation and Harmonic Suppression for Industrial Power Systems Using Thyristor Converters", IEEE Transactions on Industry Applications, Vol. IA-12, No. 3, May/June 1976, pp. 232-254.

8. T. Subbarao and J. Reeve, "Harmonics Caused by Imbalanced Transformer Impedances and Imperfect Twelve-Pulse Operation in HVDC Conversion", IEEE Transactions on Power Apparatus and Systems, Vol. PAS-95, No. 5, September/October 1976, pp. 1732-1735.

9. Teruo Kataoka, Kazuhiro Mizumachi and Shota Miyairi, "A Pulse-Width Controlled AC to DC Converter to Improve Power Factor and Waveform of AC Line Current", IEEE Transactions on Industry Applications, Vol. IA-15, No. 6, November/December 1979, pp. 670-675.

10. Tokuo Ohnishi and Hiroshi Okitsu, "A Novel PWM Technique for Three Phase Inverter/Converter", IPEC-Tokyo 1983, pp. 384-395.

11. Hasmukh S. Patel and Richard G. Hoft, "Generalized Techniques of Harmonic Elimination and Voltage Control in Thyristor Inverters: Part I - Harmonic Elimination", IEEE Transactions on Industry Applications, Vol. IA-9, No. 3, May/June 1973, pp. 310-317.

12. P.D. Ziogas and P. Photiadis, "An Exact Input Current Analysis of Ideal Static PWM Inverters", IEEE Transactions on Industry Applications, Vol. IA-19, No. 2, March/April 1983, pp. 281-295.

13. P.D. Ziogas, S. Manias and E. Wiechmann, "Application of Current Source Inverters in UPS Systems", IEEE-IAS-1983 Annual Meeting, pp. 949-957.

14. Paresh C. Sen and G. Premchandran, "Improved PWM Control Strategy for Inverters and Induction Motor Drives", IEEE Transactions on Industrial Electronics, Vol. IE-31, No. 1, February 1984, pp. 43-50.

15. S.B. Dewan and A. Straughen, "Power Semiconductor Circuits", John Wiley & Sons, 1975.

16. P.C. Sen, "Thyristor DC Drives", John Wiley & Sons, 1981.

17. P.D. Ziogas, "Optimum Filter Design for a Single Phase Solid State UPS System", Master's Thesis, Toronto University, 1975.

18. Prakash H. Nayak and Richard G. Hoft, "Optimizing the PWM Waveform of a Thyrsitor Inverter", IEEE Transactions on Industry Applications, September/October 1975, pp. 526-530.

19. R.M. Kerchner and G.F. Corcoran, "Alternating Current Circuits", Toppan Company Ltd., 1960.

20. Data Sheet of GEF90B, Hitachi Ltd., Japan, 1981.

21. Paresh C. Sen and S.R. Doradla, "Evaluation of Control Schemes for Thyristor-Controlled DC Motors", IEEE Transactions on Industiral Electronics and Control Instrumentation, Vol. IECI-25, No. 3, August 1978, pp. 247-255.